Columbia University in the City of New York | *New York, N.Y. 10027*

DEPARTMENT OF GEOGRAPHY

International Affairs Building
420 West 118th Street

(E82-10378) APPLICATION OF DIGITAL ANALYSIS OF MSS DATA TO AGRO-ENVIRONMENTAL STUDIES Semiannual Progress Report, 1 Jan. - 31 Dec. 1981 (Columbia Univ.) 99 p HC A05/MF A01 CSCL 02C G3/43

N82-32800

Unclas
00378

APPLICATION OF DIGITAL ANALYSIS OF MSS DATA TO AGRO-ENVIRONMENTAL STUDIES

Semi-Annual Progress Report
For the Period Jan. 1 - Dec. 31, 1981
NASA Cooperative Agreement NCC 5-20

Principal Investigators

Robert A. Lewis
Samuel N. Goward

CONTENTS

I. Introduction

Since 1975 members of the Department of Geography, Columbia University, have worked with NASA scientists at the Goddard Institute for Space Studies (GISS) on research concerned with satellite remote sensor observations of earth resources. This activity is currently supported under NASA Cooperative Agreement NCC 5-20. During 1981 research activities have concentrated in four areas;

1) Simulation of Landsat D Thematic Mapper (TM) observations from aircraft multispectral scanner data and field spectrometer data collected over a corn-soybeans agricultural region in Webster County, Iowa during the 1979 growing season in support of the NASA/AgRISTARS program;

2) Analysis of the simulations to evaluate the potential utility of the TM band 5 (1.55 -1.75 μm) mid-infrared observations in corn-soybeans discrimination;

3) Analysis of current Landsat data to study snow cover in northern New England and wetlands in Nebraska and Vermont in cooperation with scientists at the U.S. Army Corps of Engineers Cold Regions Research Laboratory;

4) Application of satellite remote sensor data in selected additional agro-environmental research areas pertinent to Columbia staff interests.

Dr. Samuel N. Goward, research associate, and Professor Robert Lewis, chairman of the Geography Department, are the principal investigators. Dr. Goward serves as the research director. Professor Leonard Zobler supports the activity as faculty advisor. Columbia University students work on projects under investigation as research assistants and aides. During 1981 five graduate students were funded under the cooperative agreement. Several other students, funded from other sources, also supported the research activities.

The research activities are carried out at the Goddard Institute for Space Studies. The Institute provides work space, data, computer facilities, and software to support the research. The Columbia staff interact daily with the NASA scientists to carry out the Earth Resources Group research activities. Principal GISS contacts are Dr. Stephen Ungar and Dr. Richard Kiang. Senior Columbia staff collaborate with the NASA scientists to plan and direct the research activities. The research assistants and aides participate in the research and provide technical support in preparation of presentations and reports.

II. Research Activities

A. Simulation of Landsat D Thematic Mapper Observations

In the third quarter of 1982, NASA plans to launch Landsat D. A new observing system, the Thematic Mapper, will be flown on this mission. Thematic Mapper represents a significant technical advance compared to the current Landsat observing system (J.L. Engel, 1980). A comparison of relevant TM and MSS parameters is given in Table 1. Considerable prelaunch research activity is underway to evaluate the potential information gain TM data will bring to earth resources observations (ORI, 1981). Columbia/GISS Earth Resources scientists are contributing to these activities through analysis of field measurements data collected at AgRISTARS "supersites".

The AgRISTARS field measurements program collects Landsat and ground observations at 300 selected agricultural sites across the United States (AgRISTARS, 1981). In addition, at two "supersites" (Webster County, Iowa for corn and soybeans and Cass County, North Dakota for small grains) more intensive observations are collected by the helicopter-based field spectrometer system (FSS), the NS001 aircraft-based multispectral scanner system and by ground observers. (For a discussion of the analogous LACIE field

TABLE 1

Comparison of Landsat MSS and Thematic Mapper
Sensor Specifications

	LANDSAT		THEMATIC MAPPER	
	Band #	Spectral Interval (μm)	Band #	Spectral Interval (μm)
Spectral Resolution	1	0.50-0.60	1	0.45-0.52
	2	0.60-0.70	2	0.52-0.62
	3	0.70-0.80	3	0.63-0.69
	4	0.80-1.10	4	0.76-0.90
			5	1.55-1.75
			6	2.08-2.35
			7	10.40-12.50
Spatial Resolution	80 meters		30 meters 120 meters Band 7	
Radiometric Resolution	2^6 (64 gray levels)		2^8 (256 gray levels)	

measurements program see Bauer, et al. 1978.) The supersites consist of 5 x 6 nautical mile regions in which 80 fields are periodically observed by field enumerators (NASA-USDA/ESS, 1979). These observations are timed to coincide with Landsat overpasses and are conducted at a 9 to 18 day interval. The helicopter and aircraft observations are also conducted at the same time although the aircraft is flown less frequently (once in 1979, 4 times in 1980 and 1981). The aircraft and Landsat observations provide multispectral scanner data for the entire site. The helicopter FSS observations are non-imaging high spectral resolution radiance measurements from a flight path across each of the 80 periodically observed fields.

The Conceptual Framework of the GISS Simulations

During 1981, the Columbia/GISS Earth Resources Group, as part of their AgRISTARS research effort, have developed techniques to simulate TM observations from the field measurements data. The satellite, aircraft, and helicopter observations serve complimentary roles in the TM simulation. As shown in Figure 1, the aircraft data serve as a means to simulate both TM and Landsat observations. The Landsat simulation may be compared to the real Landsat data to confirm the simulation technique. The FSS data serve as a calibration standard to verify radiometric adjustment procedures, and as the basis for extending the aircraft observations to satellite observing conditions through simulation of atmospheric effects and consideration of the satellite TM engineering parameters. In addition, the FSS observations permit temporal evaluation of crop radiance behavior in TM bands at those times when the aircraft is not flown.

The GISS-developed techniques include radiometric, geometric, and resolution processing of the aircraft scanner data and radiometric and statistical processing of the FSS data. These techniques were tested using

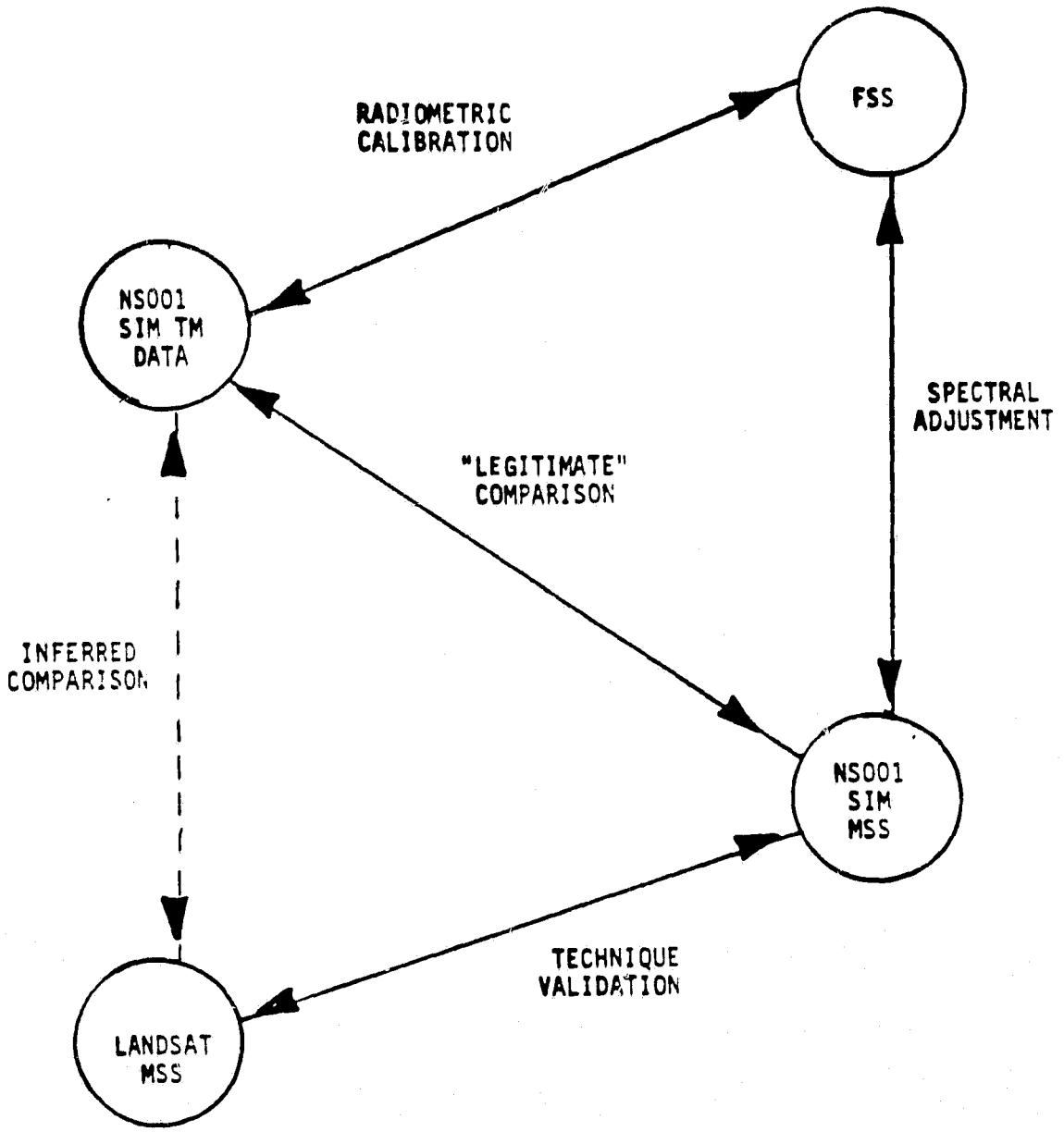

FIGURE 1 TM SIMULATION APPROACH

From Presentation material used by S. Ungar; Renewable Resources Thematic Mapper Simulator Workshop (ORI, 1981).

1979 field measurements data from the Webster County, Iowa supersite (Figure 2). One NS001 flight, collected on 8/30/79 and four FSS observations collected on 6/11, 6/29, 7/16, and 8/30/79, were processed to simulate TM observations.

TM Simulations From NS001 Data

The NS001 (NASA scanner 1) instrument was constructed by NASA engineers at the Johnson Space Center to emulate, as much as possible, the satellite TM instrument (Richard, Merkel and Meeks, 1978). The NS001 instrument parameters are given in Table 2. The NS001 is typically flown on the NASA C-130 aircraft at altitudes between 5 and 8 kilometers. With a 2.5 milliradian detector IFOV, the scanner observes, at nadir, a 19 meter square ground resolution element from 7,620 meters (25,000 feet) altitude. At this altitude, the scanner normally operates at 15 revolutions per second which, for the nomimal aircraft ground speed of 135 meters/sec, produces a 50% overlap between adjacent scan lines. As the instrument was constructed prior to final selection of TM bands, eight rather than seven bands are included in the detector package (NS001 band 5, 1.00 - 1.30 μm is the non-TM band).

Although the NS001 scanner was constructed to emulate the satellite TM scanner, no aircraft scanner system is fully capable of simulating satellite observing conditions. Not only does the aircraft fly at much lower altitudes, thus not observing the full effects of atmospheric attenuation, but also, because of the altitude difference, the scanner must observe the surface at more extreme scan angles to view a ground area comparable to a small subarea in one satellite scene (ORI, 1981).

The NS001 maximum scan angle from nadir is 50 degrees. This permits the instrument to view an across track ground swath of 18 kilometers (± 9 kilometers from nadir) at an altitude of 7,620 meters. This variation in look

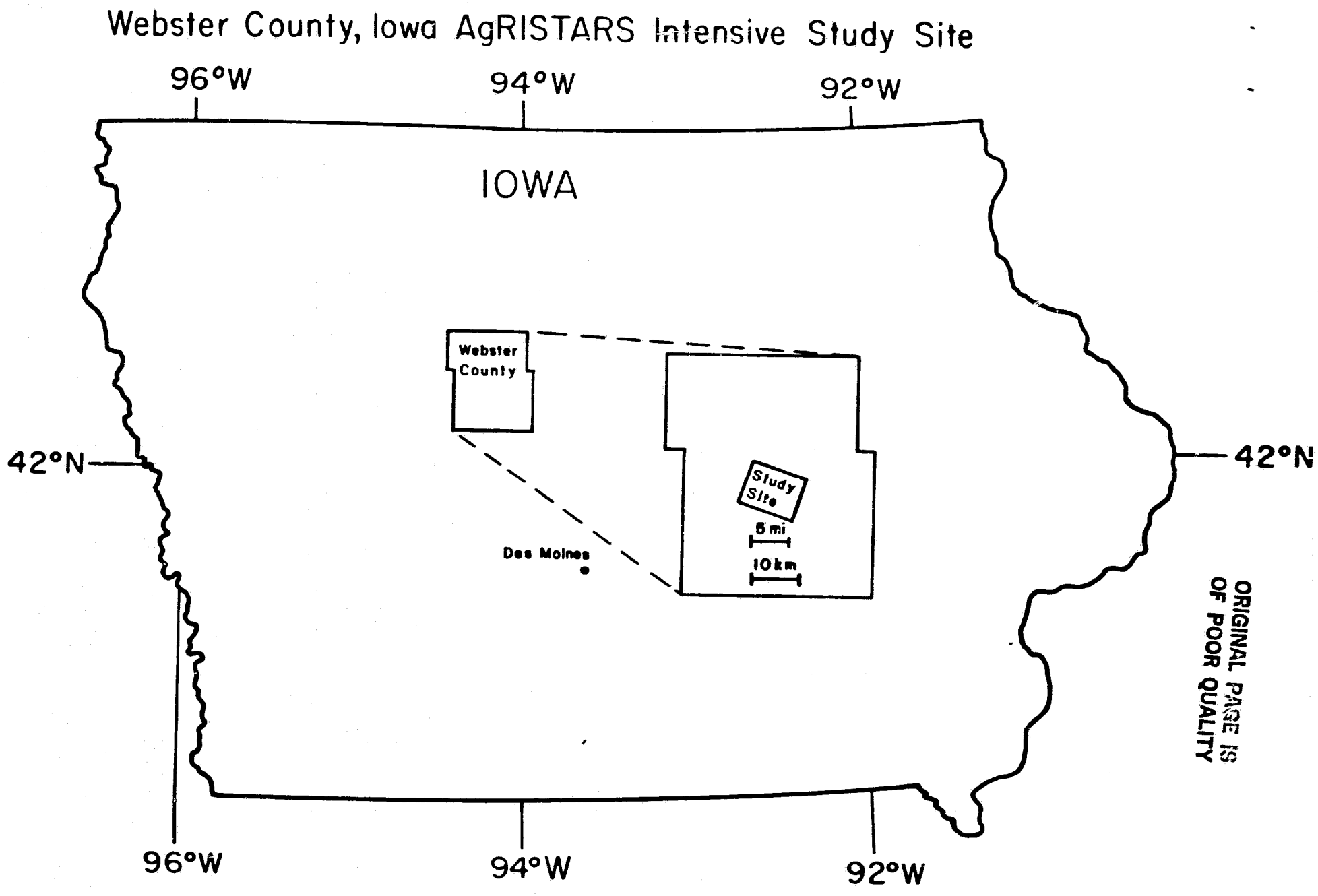

FIGURE 2

TABLE 2

NS001 TECHNICAL SPECIFICATIONS

SPECTRAL BANDS

Band	Detector	Spectral bandwidth, μm	NE'P, %
1	S_i	0.45 - 0.52	0.5
2	S_i	0.52 - 0.60	.5
3	S_i	0.63 - 0.69	.5
4	S_i	0.76 - 0.90	.5
5	G_e	1.00 - 1.30	1.0
6	G_e	1.55 - 1.75	1.0
7	I_nA_s	2.08 - 2.35	2.0
8	HgCdTe	10.4 - 12.50	NEΔT = 0.25°K

DESIGN DATA

Instantaneous field of view (IFOV)	2.5 × 2.5 milliradians
Across-track field of view	100°
Nominal aperture diameter	10.16 cm
Effective aperture area	72.4 cm^2
f number	1.85
Primary focal length	18.8 cm
Inflight calibration	Integrating sphere and two controllable blackbodies
Short wavelength array temperature	198°K
V'H range	Variable 0.025 to 0.25
Scan rate	Variable 10 to 100 scans/sec
Scan speed stability	One-third of the IFOV, scan line to scan line
Data quantization	8 bits (256 discrete levels)
Number of video samples/scan line	700
Roll compensation	±15°
Data format	Compatible with M^2S
Scan mirror	45° rotating mirror
Tape packing density	10 000 bits-per inch (BPI) constant
Recording code	Bi-Φ-L

angle introduces significant across track variations in ground resolution and the radiometric conditions observed by the sensor that will not be present in the TM observations.

An additional factor, which should not be present under satellite conditions, is complex distortion of image geometry due to short term changes in aircraft motion. At 8,000 meters altitude, the C-130 aircraft is subject to uncontrolled motion due to buffeting in the turbulent lower atmosphere. Short term changes in the velocity, altitude, pitch, yaw and roll of the aircraft can significantly alter the geometry of the image data in comparison to satellite observations (and other information available such as photography and maps). The NS001 is roll-compensated (Richard, Merkel, and Meeks, 1978) However, other motions of the aircraft during data acquisition significantly affect the image geometry. Figure 3 presents a grayscale image of raw NS001 Band 6 (TM5) data from 8/30/79 which displays the resolution, radiometric and geometric prperties of a typical aircraft scanner image.

Aircraft Scanner Data Processing Techniques Developed

Although processing techniques developed by the Columbia/GISS staff were specifically directed to processing the NS001 data, these same techniques are applicable to aircraft scanner data from other systems such as the NASA/ERL TM simulator and the NASA/Ames Daedalas system. The approach is to develop techniques, where possible, that systematically account data variations introduced by the scanner system. For example, ground resolution variations are, in general, an explicit function of scan angle. However, certain characteristics of the data must be treated empirically. Variations in atmospheric optical depth, scattering, and surface bidirectional reflectance, although they appear to be related to scan look angle, are not sufficiently known to be subject to systematic correction. In this case, empirical

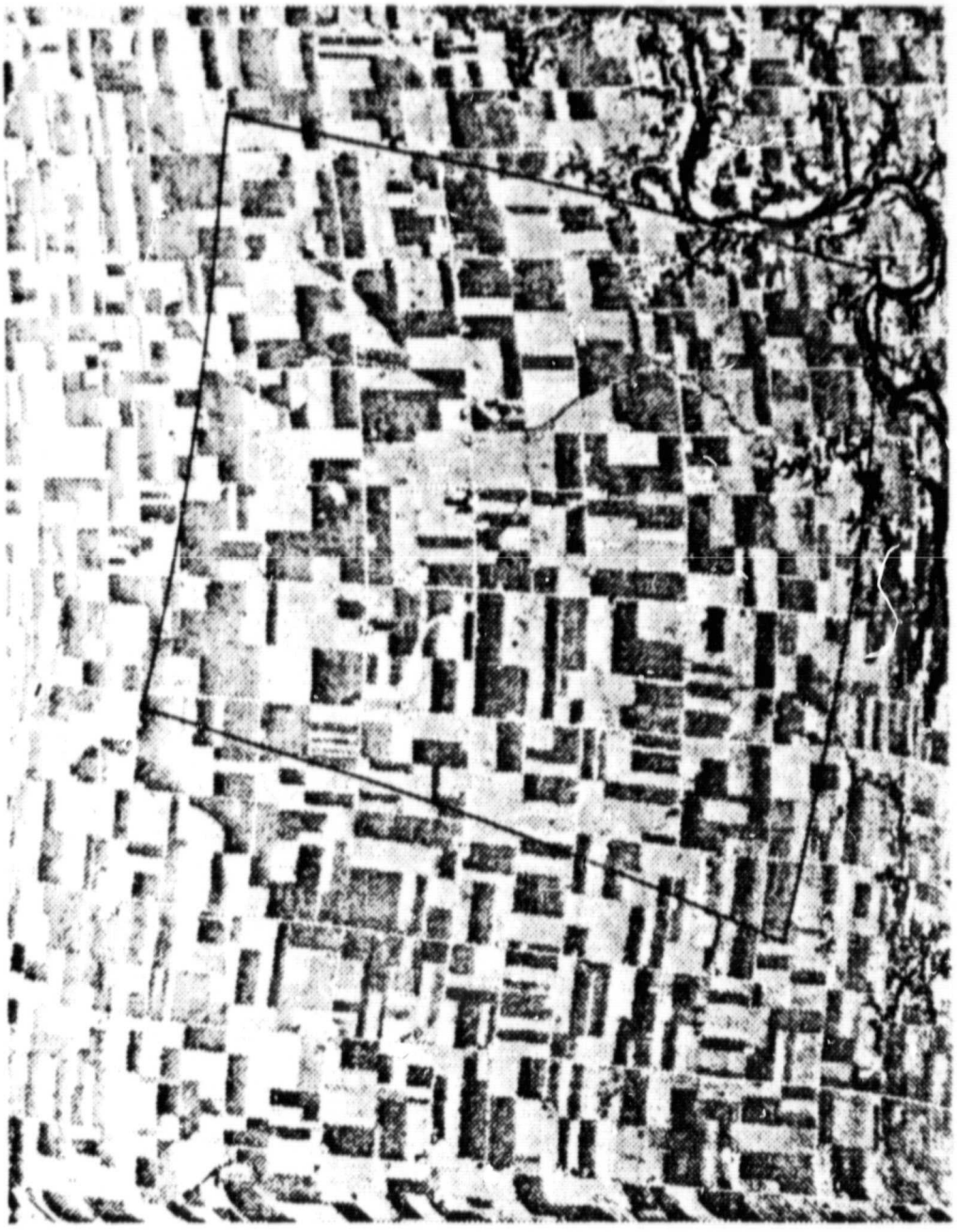

WEBSTER Co. 8/30/79 NS001
1.55 - 1.75 μm

FIGURE 3

techniques were developed to compensate or adjust the data in a reasonable fashion. Correction of the effects of platform velocity, altitude and attitude variations on image geometry presents a particularly difficult problem. Although systematic techniques are possible, practical implementation requires a high quality source of aircraft navigational data during scanner observations. Under relatively stable flight conditions, empirical "rubbersheeting" techniques appear to be adequate. However, under unstable flight conditions a more systematic approach is needed. Expermental activities in both areas were explored by the Columbia/GISS group in 1981.

Ground Resolution

Whereas the NS001 ground resolution is 19 meters at nadir from a 7,620 meter altitude, at the 50 degree maximum look angle, the ground resolution element is approximately 30 meters in the along track direction by 46 meters in the across track direction. Since the NS001 instrument is roll-compensated and pixels are contiguous in the scan direction, calculation of the scan angle position of each pixel in a scan line is straight forward. The central pixel in each scan line represents the nadir pixel, each adjacent pixel is 2.5 milliradians of scan angle away from nadir. The ground resolution of any pixel in the scan may be calculated by (Baker and Mikhail, 1975):

$$R_{\text{along track}} = (h/\cos A)a \qquad (1.1)$$

$$R_{\text{across track}} = (h/\cos^2 A)a \qquad (1.2)$$

where R = linear resolution
h = altitude
A = look angle
a = angular resolution of the detector.

To aid in later geometric processing, the data are resampled to nominal 10 meter pixels. In the scan direction resampling is conducted using equation 1.2. Since adjacent scans are 50% overlapped each scan is assumed to

represent a 10 meter data sample. After geometric correction the 10 meter pixels are aggregated to 30 meter pixels to simulate the nominal satellite TM ground resolution. Figure 4 is a grayscale of the 8/30/79 NS001 band 6 (TM band 5) data which has been resampled to 10 meters and radiometrically adjusted.

Radiometric Adjustment

Because the NS001 makes observations to 50 degrees either side of nadir the radiance measured varies not only as a function of the ground cover present but also due to the bidirectional radiance properties of the ground cover, variations in atmospheric path length and anisotrophic scattering of the radiant flux by atmospheric aerosols. The relation between incident solar radiation and the NS001 maximum look angles for the 8/30/79 observation is plotted in Figure 5. Note that the solar flux is nearly perpendicular to the eastern look angle and nearly parallel to the western look angle. Figure 6 is a plot of the mean and standard deviations for each column of the western portion of the 8/30/79 NS001 band 1 (0.45 - 0.52 μm) data. The general pattern displayed is increasing radiance with increased westerly look angle; less significant variations occur in the easterly direction. The reduced canopy shadowing and increased canopy cover along with increased observed aerosol scattering due to both increased path length and increased back scatter parallel to incident solar illumination, cause the image to brighten in the westerly direction.

The Column-Averaging Approach

The landscape and atmospheric conditions that contribute to this effect are not sufficiently known to explicitly compensate for their variation as a function of look-angle. A simple empirical approach to radiometric

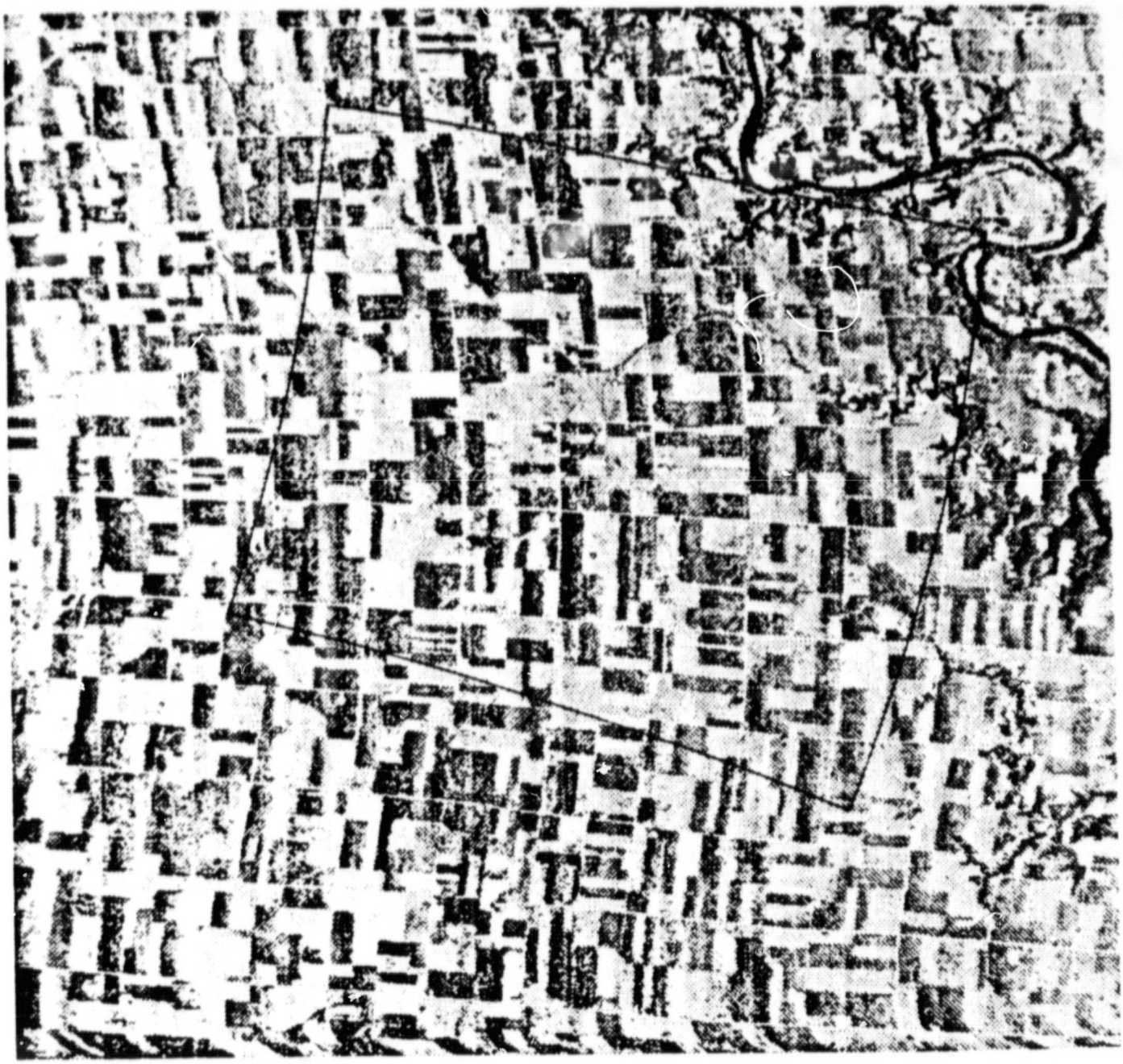

SCAN-ANGLE ADJUSTED

FIGURE 4

AgRISTARS INTENSIVE STUDY SITE
WEBSTER COUNTY 8-30-79

NSOOI FLIGHT LINE I
SUN/LOOK ANGLE

10:10 LOCAL TIME
SUNEL = 46°
AZ = 131°

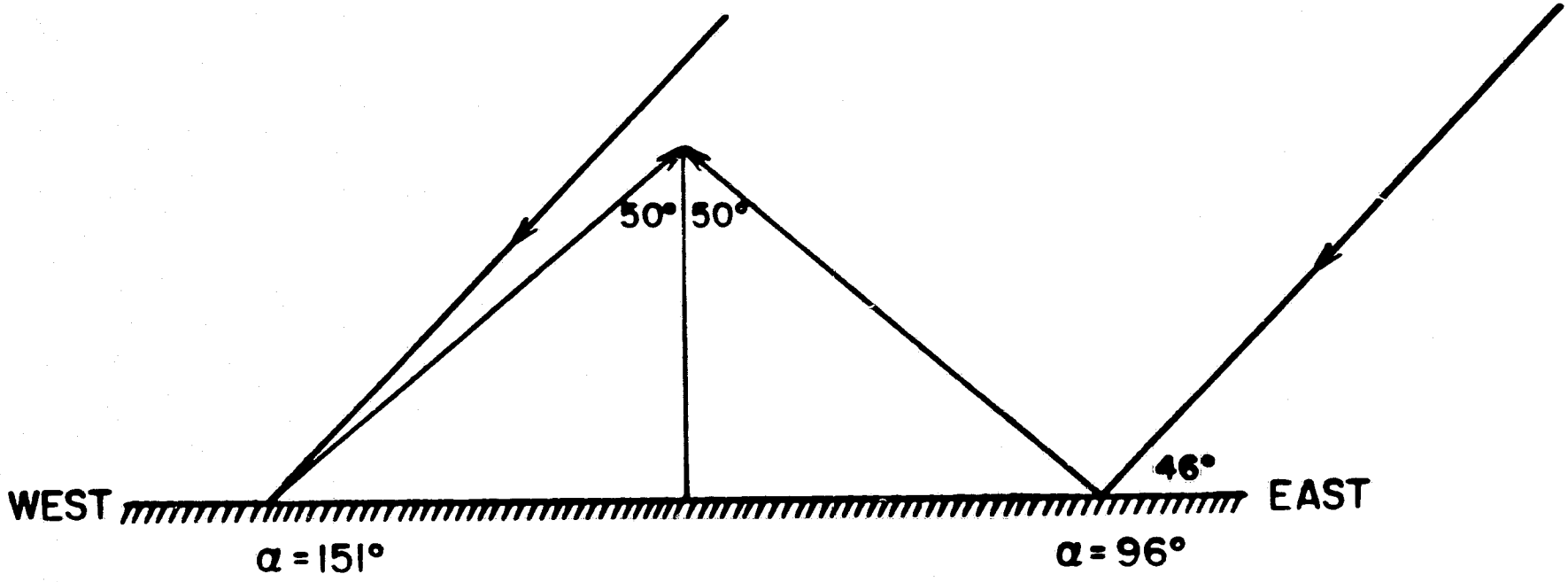

FIGURE 5

PLOT OF COLUMN MEANS ± 1 S.D.

AND SCAN-ANGLE ADJUSTMENT

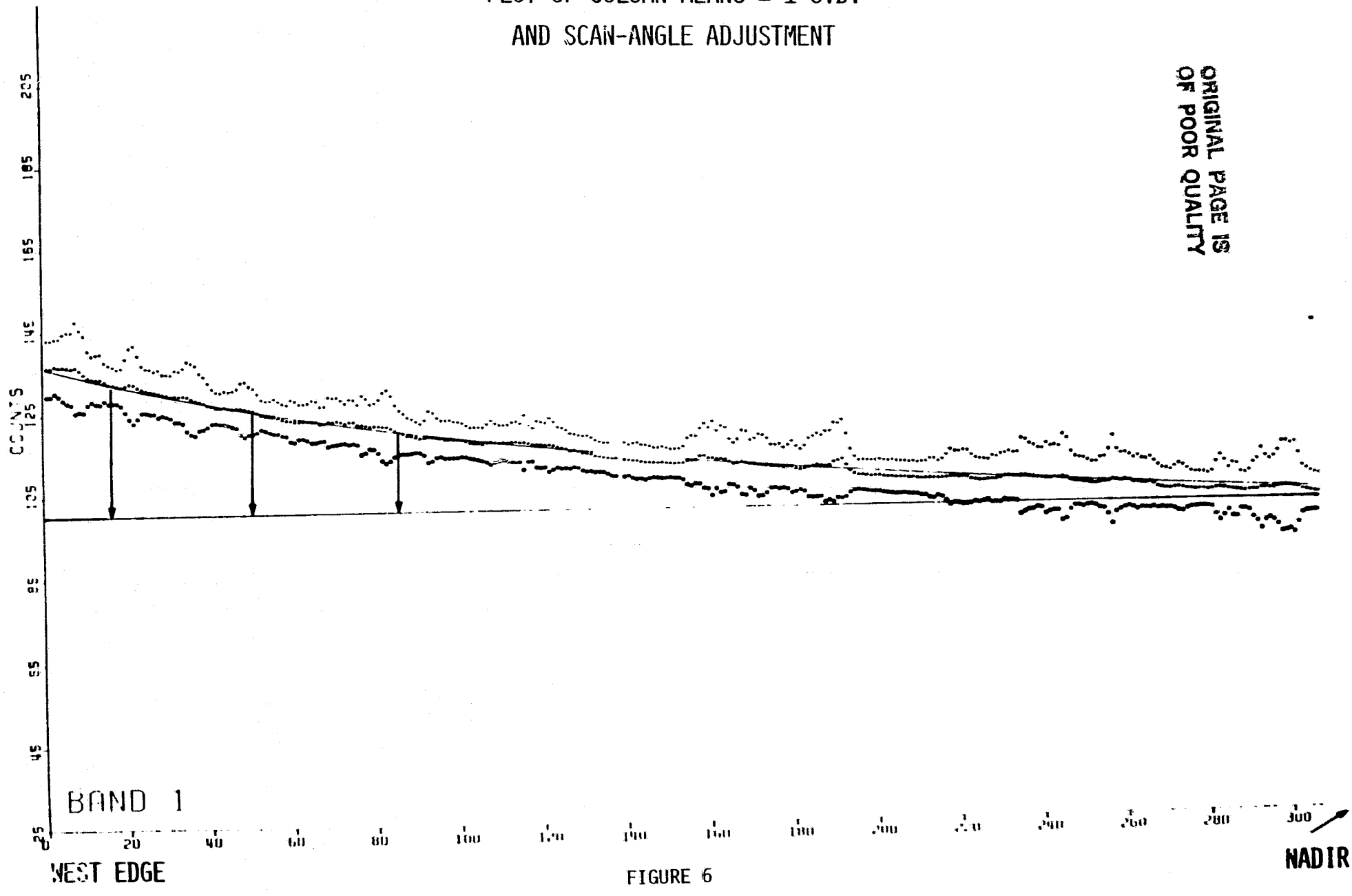

FIGURE 6

adjustment, which will insure a uniform tonal distribution across the image, is to derive a least-squares fit to the column-average distribution. As shown in Figure 6, this least-squares line can be used to calculate a column-by-column adjustment of the data that produces the uniform tonal appearance of the image data displayed in Figure 4.

The assumptions that underlie this column-average radiometric adjustment approach are that landscape materials of differing reflectance properties are randomly distributed in the scan direction and that the bidirectional reflectance of the landscape is independent of landscape type (e.g., corn and soybean canopies). From visual inspection of the 8/30/79 NS001 data the former assumption is reasonably satisfied for this data set. The latter assumption was statistically examined for the 8/30/779 data.

Following the classification procedures discussed later in this report, the radiometrically adjusted data were classified, on 0% commission error basis, to identify corn and soybeans pixels. The classification map was used as a mask on the raw data to select corn and soybeans pixels. Data column-averages and least-squares fits were then computed independently for corn and soybeans. Any difference in the corn and soybeans column average patterns would suggest differential corn/soybeans bidirectional reflectance as a function of look angle. Visual inspection of the comparable corn/soybeans plots revealed little difference in the two curves. Statistical evaluation of the least-squares fits indicated that there is a slight but statistically significant difference. Thus, although differences in corn and soybean canopies during this 8/30/79 observation appear to differentially effect the column-average pattern of the data, the difference is small and can be, for this data set, ignored.

Comparison of Radiometrically Adjusted NS001 Data and FSS Observations

The FSS observations may be used as an independent check of the radiometric adjustment procedure. The FSS instrument acquires nadir observations of the same ground area the NS001 scans. FSS data are processed to NS001 sprectral band intervals (see "TM Simulations from FSS Data"). By comparing the two data sets before and after NS001 data radiometric adjustment the effectiveness of the adjustment may be evaluated.

The locations of the helicopter flightlines were derived by analysis of the FSS boresight color photography and CIR photography acquired during the NS001 overflight. The FSS instrument, when flown at 60 meters, observes a nominal 24 meter spot size (Bauer et al., 1978). However, one rotation of the filter wheel takes about one second, during which time the helicopter moves approximately 27 meters with respect to the ground. To select equivalent NS001 observations every other NS001 pixel along the helicopter flightline was extracted from the NS001 data. The mean value per field of the FSS and NS001 data were correlated to study the impact of the radiometric adjustment procedure.

Table 3 presents the results from the correlation analysis. Correlations between the two data sets prior to adjustment are consistently lower than following adjustments. This indicates that radiometric adjustment makes the NS001 data appear more like nadir observations. The relation, after adjustment for all crops shows a strong relation ($R^2 > 0.9$) between the two data sets. Correlation between corn and soybean means taken separately shows somewhat lower final R^2 values. This is most likely the result of low within-crop variability in the reflectance of corn and soybean canopies, close to the sensitivity limits of the two instruments. However, the differential bidirectional reflectance of the corn and soybeans canopies may also affect this relation. Scatterplots for NS001 bands 1 and 4 of the before and after

TABLE 3

CORRELATION (R^2) OF INTEGRATED FSS MEANS WITH CORRESPONDING NS001 CHANNELS

NS001 CHANNEL	RAW DATA			SCAN ANGLE ADJUSTED		
	ALL	CORN	SOY	ALL	CORN	SOY
1	0.19	0.01	0.02	0.76	0.54	0.39
2	0.47	0.02	0.44	0.92	0.61	0.92
3	0.73	0.10	0.69	0.86	0.54	0.88
4	0.87	0.36	0.56	0.95	0.68	0.82
6	0.81	0.01	0.22	0.95	0.42	0.58
7	0.50	0.00	0.13	0 .75	0.01	0.12

adjustment relations between FSS and NS001 data are given in Figure 7. These plots confirm the tabular results from the correlation analysis.

Geometric Correction

Aircraft altitude, velocity, and attitude variations during scanner observations introduce complex geometric distortions in the scanner imagery. These distortions will generally not be present in the satillite data and make comparison of the aircraft data with maps and photos of the area, as well as construction of registered temporal data sets, difficult. Two approaches, one empirical and the other systematic, to geometric correction of the aircraft scanner data have been investigated by the Columbia/GISS staff during 1981.

The empirical geometric correction approach uses map and image control points to statistically derive a "rubbersheet" transform of the image data that matches, as much as possible, the geometry of the map control point source (Baker and Mikhail, 1975). The systematic approach use aircraft altitude, velocity, and attitude information, recorded during the observation, to compensate for the effects of these variations on the image geometry (Spencer, Wolf, and Schall, 1974). Although the latter approach is more desirable, since it represents a "true" correction of these distortions rather than a statistical estimate, it is highly sensitive to the precision and accuracy of the recorded aircraft altitude, velocity, and attitude information. The experiments completed at GISS during 1981 suggest that for the current NS001 observations the empirical approach is more sucessful than the systematic approach.

FIGURE 7

COMPARISON OF FSS AND NS001 MEANS BEFORE AND AFTER NS001 RADIOMETRIC ADJUSTMENT

NS001 VERSUS INTEGRATED FSS FIELD AVERAGES
TM BAND 1 (0.45-0.52μm)

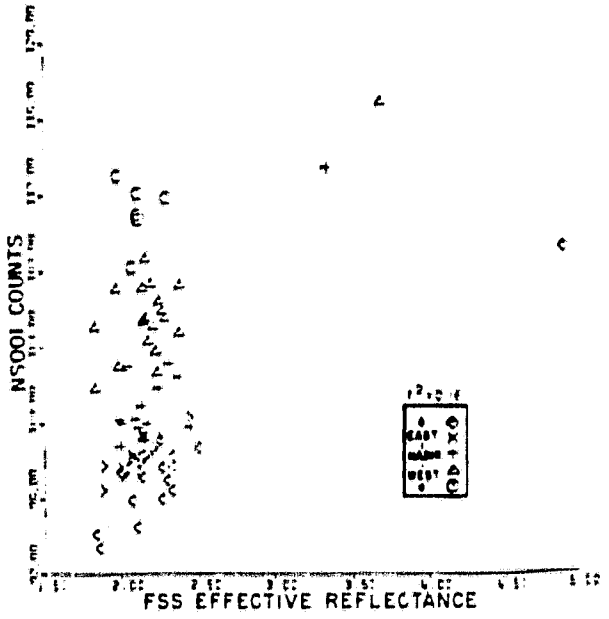

ADJUSTED NS001 VERSUS INTEGRATED FSS FIELD AVERAGES
TM BAND 1 (0.45-0.52μm)

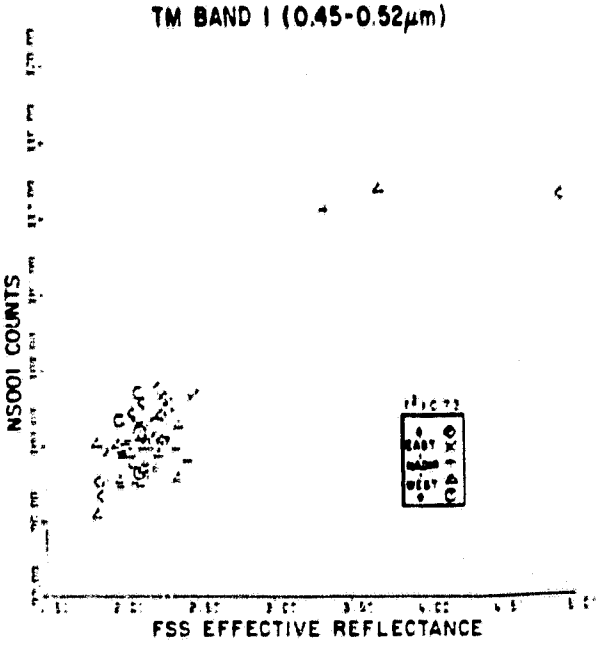

NS001 VERSUS INTEGRATED FSS FIELD AVERAGES
TM BAND 4 (0.76-0.90μm)

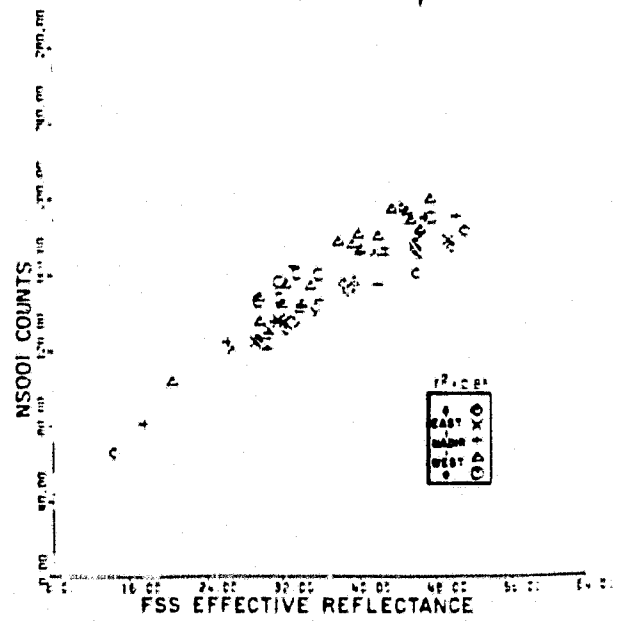

ADJUSTED NS001 VERSUS INTEGRATED FSS FIELD AVERAGES
TM BAND 4 (0.76-0.90μm)

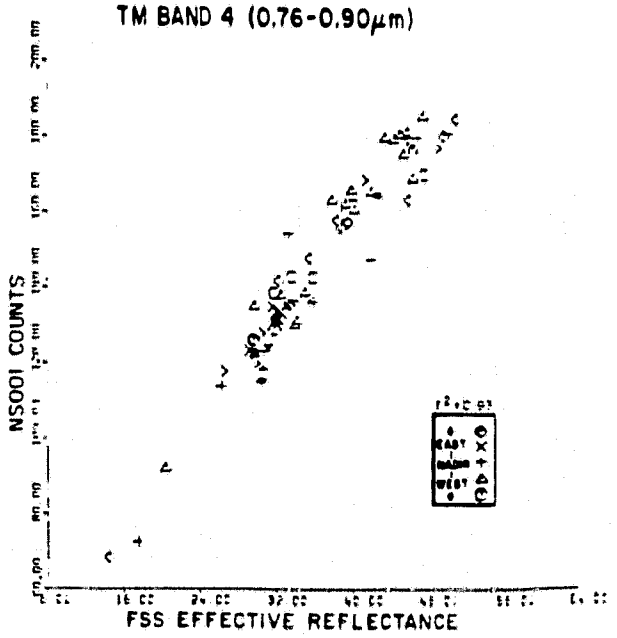

Empirical Geometric Correlation

The empirical "rubbersheet" approach to geometric correction requires a dense network of control points that can be easily located in the image data and a ground reference source. For the United States, USGS 7.5 minute quadrangles provide an accurate source of ground information. In the Webster County, Iowa, region one feature, which is common to the maps and and the image data, is the road network. The road system follows the Township and Range survey system at one mile intervals. The intersections between the N-S/E-W roads were selected as ground control points. The road intersections are uniformly distributed in the data and easily located in the maps and in the image data. To encompass Webster County supersite 59 road intersections were selected as ground control points (figure 8).

The map coordinate locations of the road intersections are derived from the USGS maps by locating the center of each intersection on the map and digitizing the locations via the flatbed digitizer at the Columbia University Lamont-Dorherty Laboratories. The digitizer table precision is 1/1000 of an inch. For the USGS 1/24,000 scale map this results in a ground coordinate location precision of better than one meter.

The image coordinates are located on line printer grayscales of the ten meter data. Preliminary experiments were conducted using grayscales of NS001 bands 3,4, and 6 to determine which band or bands were best suited for identification of the road intersections. Band 3 was found to be most effective, followed by band 6 and band 4. Two analysts, each working with a different bands, independently identified the line and column locations of the 59 road intersections in 10 meter data. The road intersection is defined as the point at which two lines, one located at the center of the N-S road and one located at the center of the E-W road, intersect in the grayscale (Figure 9). For the 8/30/79 data the two analysts generally selected the same ten

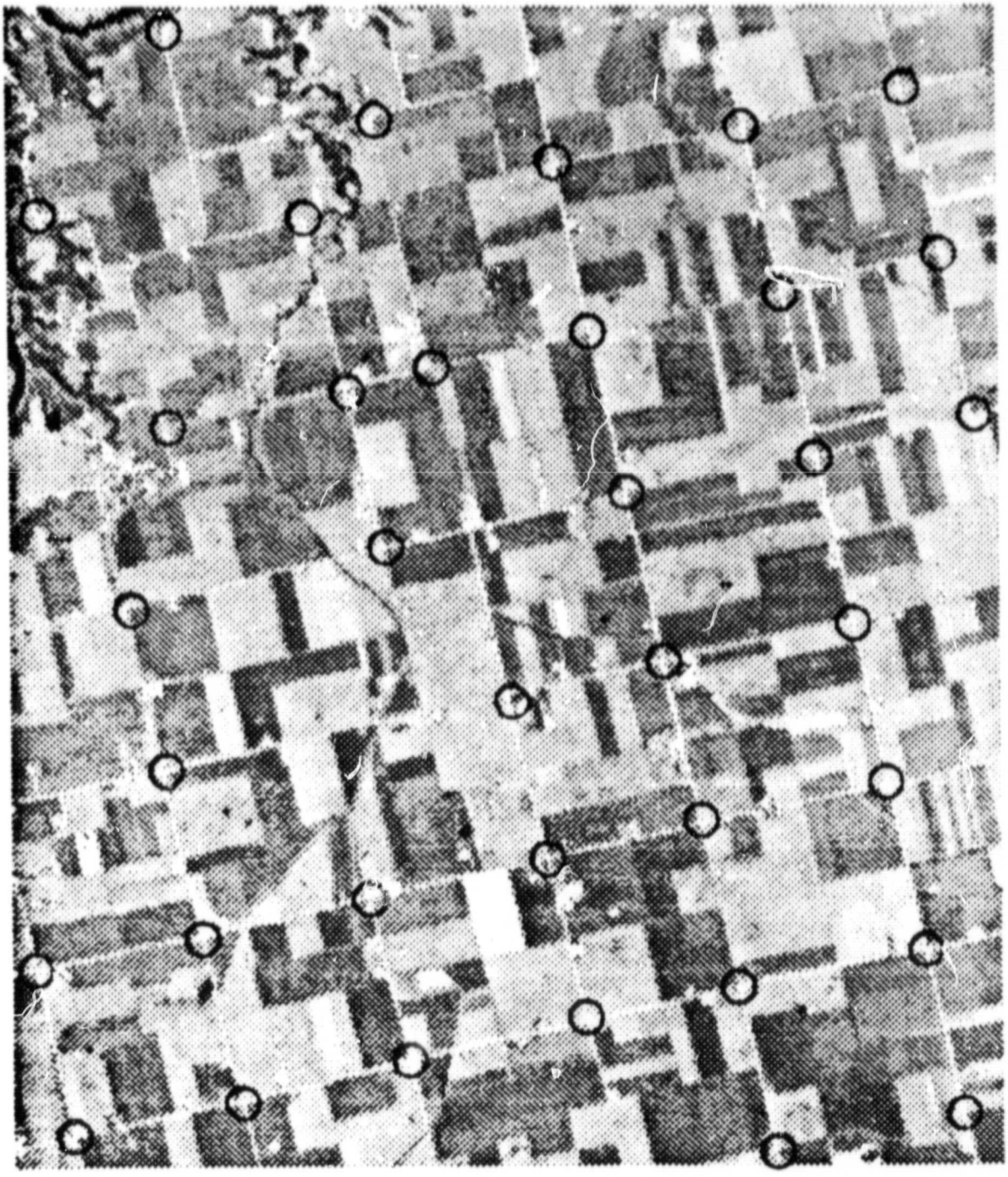

GROUND CONTROL POINTS IN WEBSTER CO. SITE

FIGURE 8

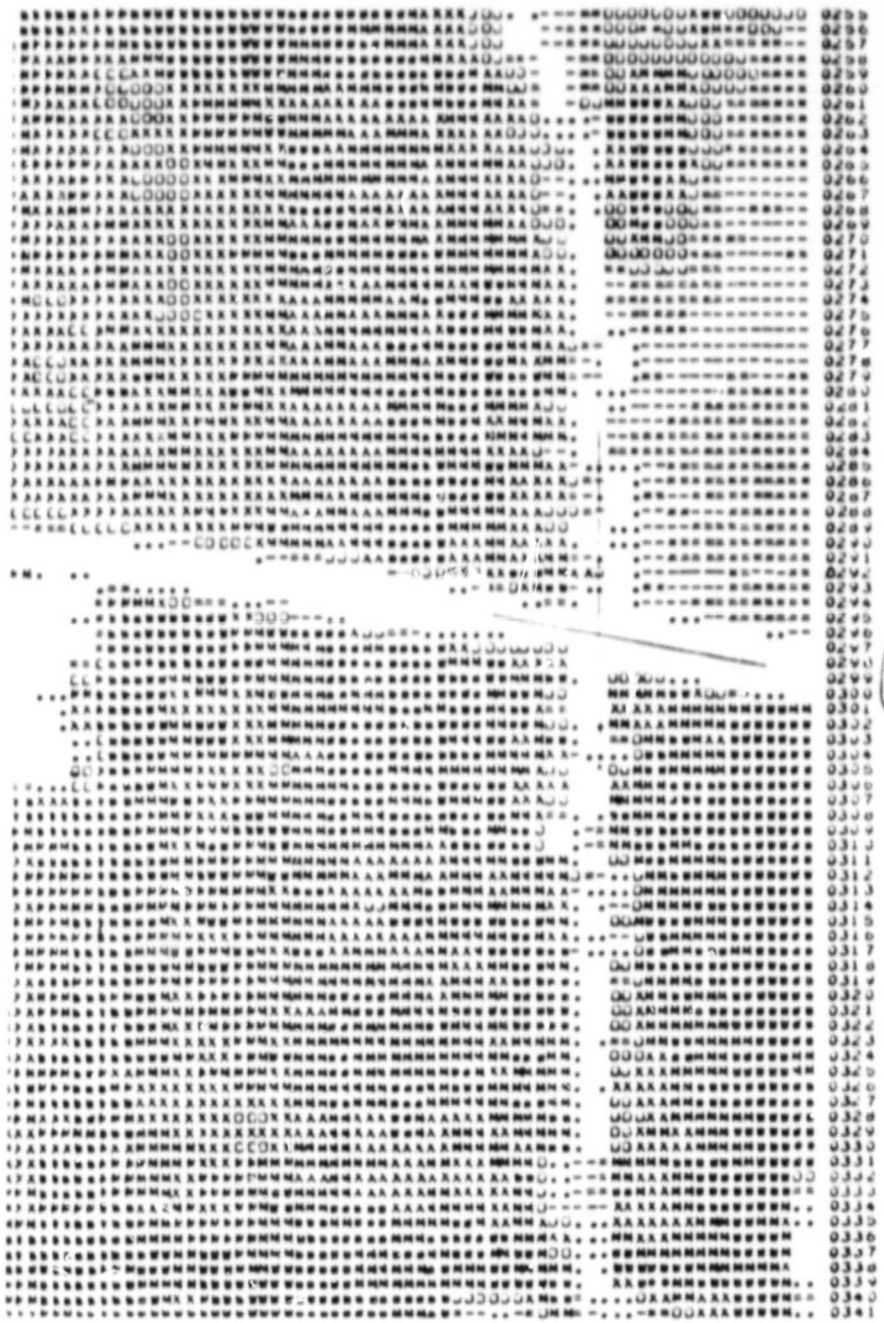

FIGURE 9

LOCATION OF A ROAD INTERSECTION IN
NS001 BAND 3 GRAYSCALE

meter pixel. In those cases where they disagreed the difference was one coordinate location in one direction only.

The rubbersheet transform is derived by calculating a least-squares polynomial relation between the image and map coordinates. The general form of the relation is:

$$x' = a_0 + \sum_{i=1}^{n} a_i \, x^i \qquad (2.1)$$

$$y' = b_0 + \sum_{i=1}^{n} b_i \, x^i \qquad (2.2)$$

where x',y' represent the map coordinates and x,y represent the image coordinates. This relation is used to reassign data from the image coordinate system to the map coordinate system. The nearest neighbor criterion is used to specify which image data are assigned to each map coordinate location.

Transformation experiments conducted with the 8/30/79 NS001 data led to the conclusion that a third order polynomial fit produces visually the most acceptable solution. Although higher order polynomials result in lower root mean square (RMS) error relations between the image and map control points than the third order, they also introduce geometric distortions in the resultant image that are not present in the raw data. The RMS error to a third order fit on the 59 control points in the 8/30/79 data is approximately 60 meters (two TM pixels).

Local Rubbersheeting

Analysis of the third-order transformed 8/30/79 data indicated that the greatest residual error was a high frequency variation of the distance between control points in the flightline direction (Figure 10); possibly due to aircraft pitch motion. Higher order polynomials had been judged ineffective. An alternate approach in this case is to rubbersheet local

FIGURE 10

RATIO OF VERSION 1 IMAGE TO MAP DISTANCES
FOR ADJACENT GCP's (IN Y DIRECTION)

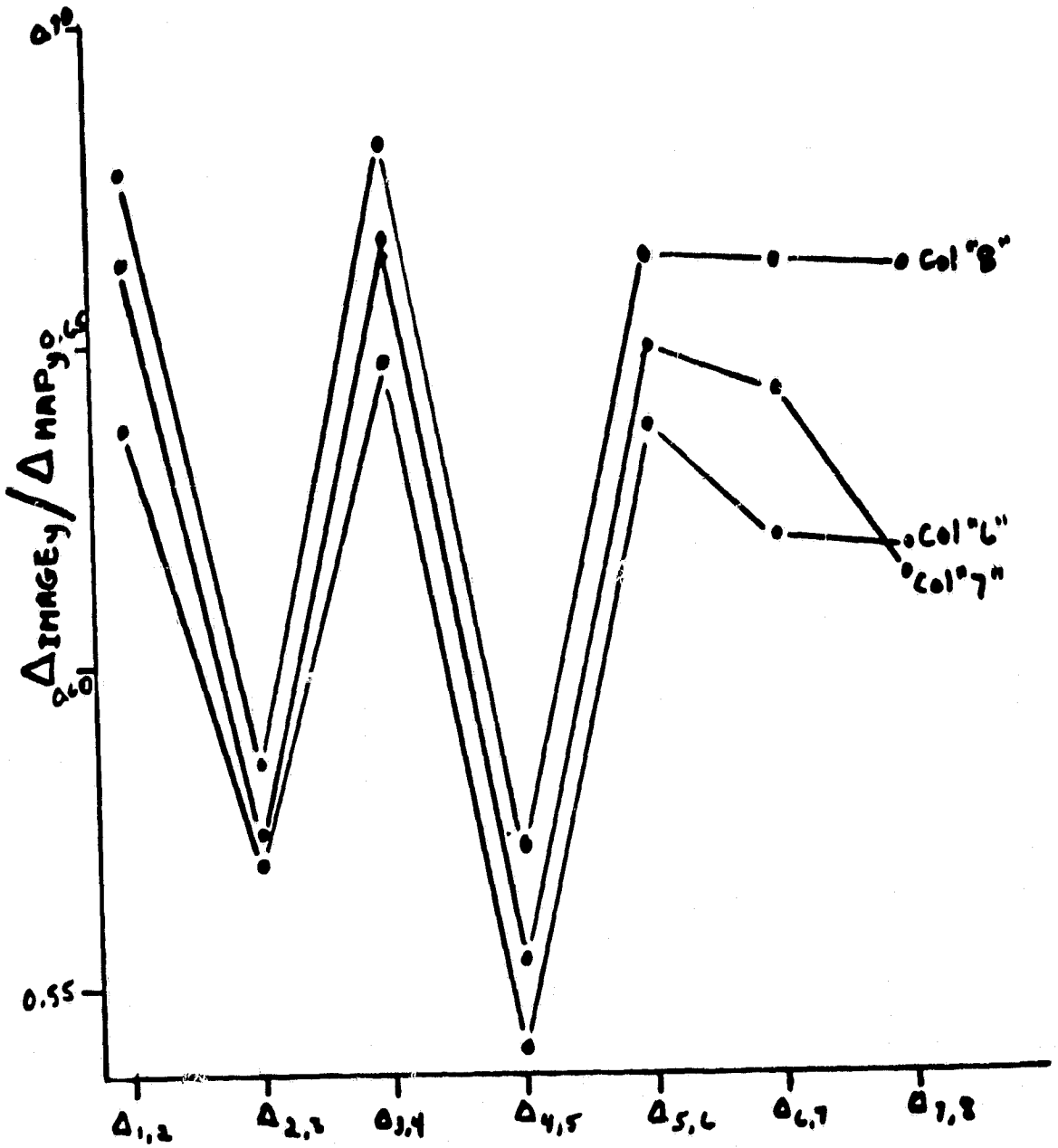

strips of the data in which this residual effect could be treated by lower order polynomials (Figure 11). To insure continuity of the image strips following transformation, the transformation of each strip is constrained to fit selected control points in adjacent strips. This insures that the transformed image strips will match at these points and, if the local transformation is reasonable, that the strips will properly mosaic. Local rubbersheeting of the 8/30/79 data produced a visually acceptable image with an average RMS error for the 59 control points of less than 10 meters (Figure 12).

Systematic Geometric Correction

Experiments with the 8/30/79 NS001 data demonstrated that the empirical rubbersheet approach to geometric correction is not well suited to aircraft scanner images where short term variations in platform motion have introduced local geometric distortions. Preliminary screening of the 1980 AgRISTARS NS001 observations indicated that this high frequency local geometric distortion is typically present in the NS001 data. The 9/10/80 flight over Webster County, Iowa presents an extreme case of this problem (Figure 13). There is a great need to establish a more systematic approach to geometric correction of aircraft scanner data which draws upon recorded aircraft motion information to correct for motion-introduced distortions.

NERDAS

The navigational parameters of the NASA C-130 aircraft are recorded during observation missions by the NERDAS (NASA Earth Resources Data Annotation System). Signals from the Litton 51 navigational computer (LTN-51), radar altimeter, and attitude sensors (pitch and roll) as well as clock time are recorded by the NERDAS (NASA, 1980). The relevant NERDAS recorded parameters and their precision is given in Table 4.

FIGURE 11
IMAGE STRIPS USED FOR LOCALLY ADJUSTED
RUBBER-SHEETING

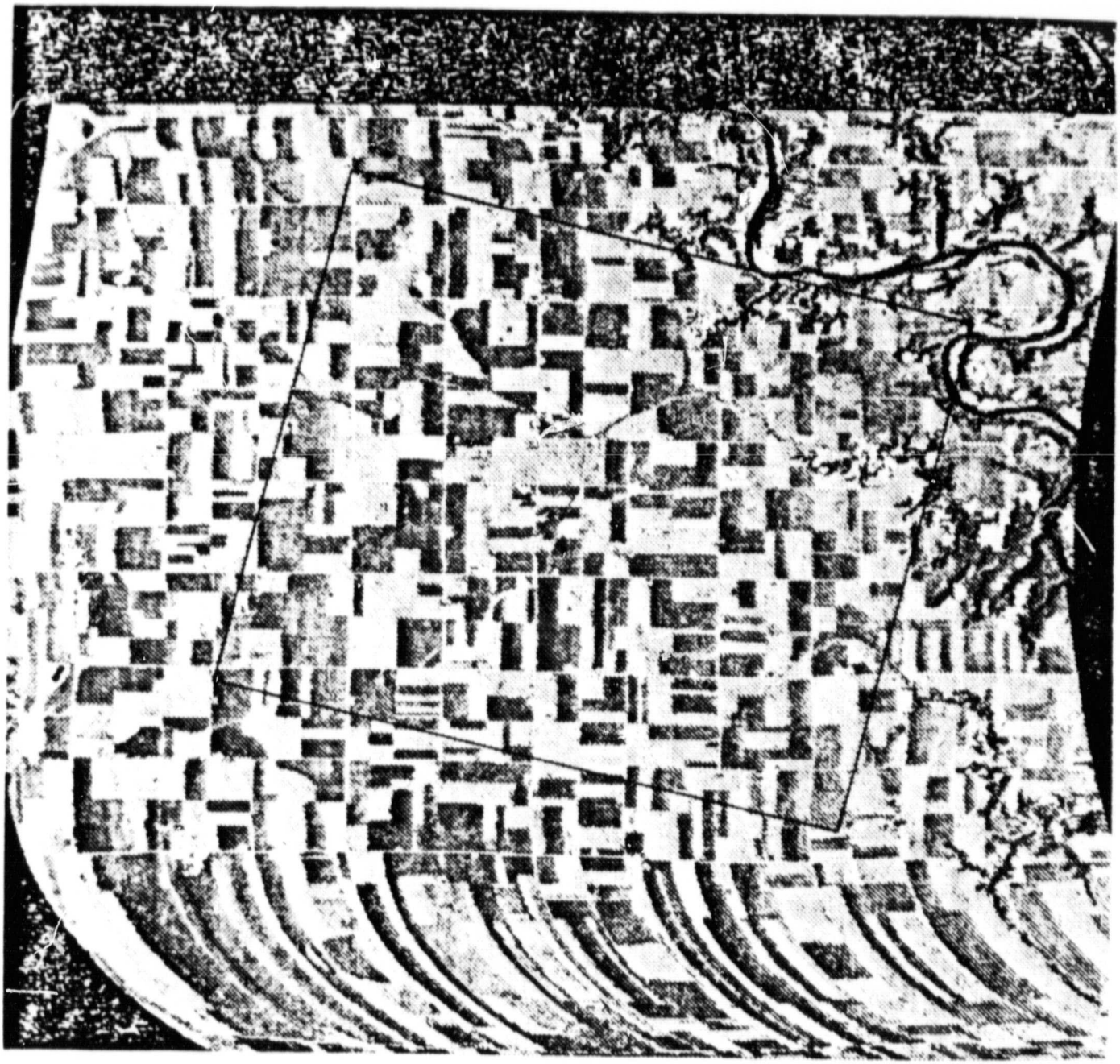

FIGURE 12

PIECEWISE RUBBER-SHEETED

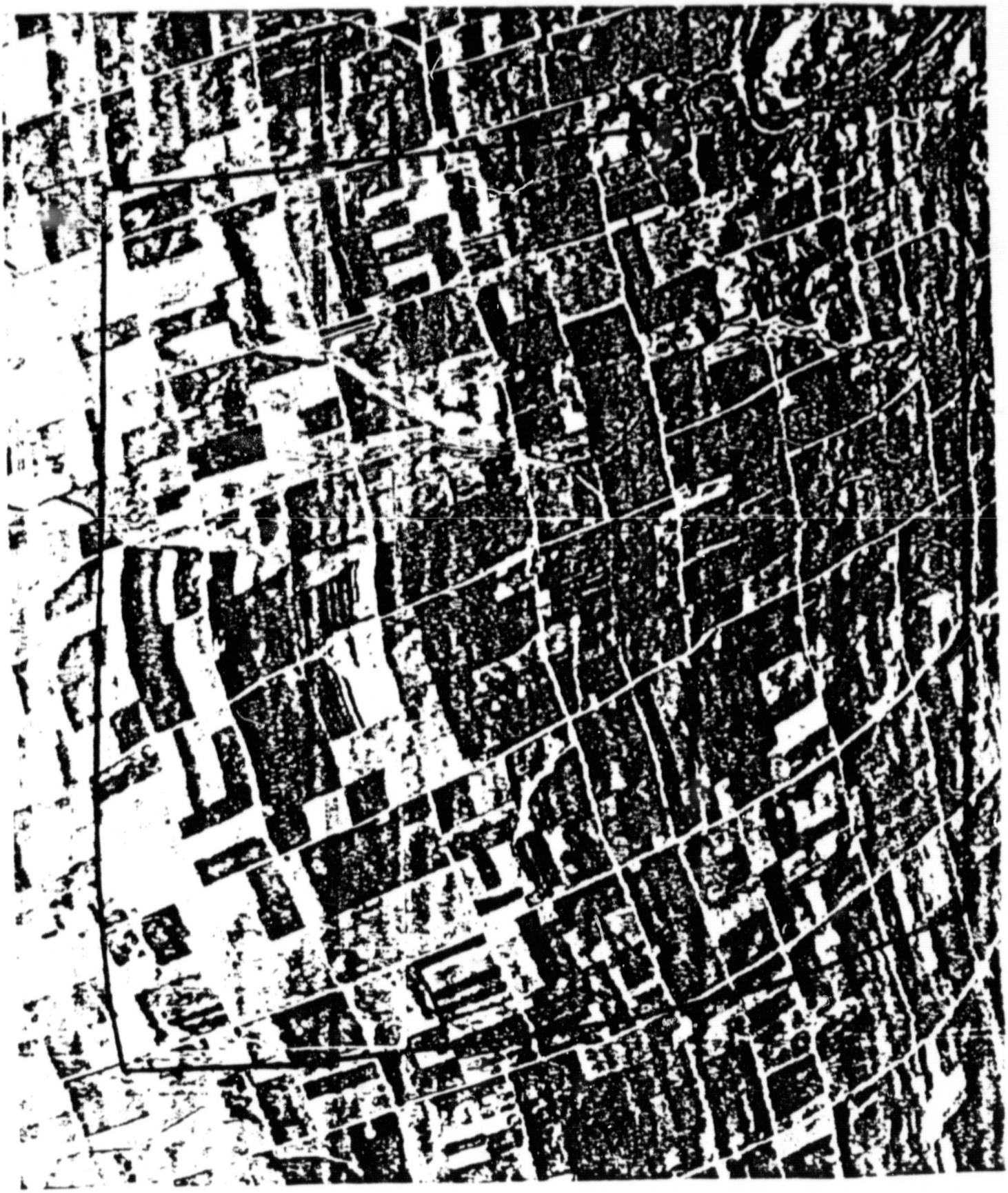

WEBSTER CO, IOWA AgRISTARS ITS NS001 SEPT. 10, 1980

FIGURE 13

TABLE 4

NERDAS-RECORDED NAVIGATIONAL PARAMETERS NEEDED
FOR SYSTEMATIC GEOMETRIC CORRECTION

PARAMETER	NERDAS PRECISION
Time	0.1 second
Altitude	10 feet
Heading	0.1°
Drift	0.1°
Roll	0.1°
Pitch	0.1°
Ground Speed	1 knot

In the ideal case the NERDAS data should be updated for each observation (pixel) of each scan. At a scan rate of 15 revolutions per second (rps) an update rate of 0.2 milliseconds would be required. Under the assumption that the aircraft is stable during one scan, an update rate of 67 milliseconds is needed at 15 rps to account for motions between scans. The NERDAS records are updated every 40 milliseconds, however individual parameters have differing update rates (Spencer, Wolfe, and Schall, 1974). In particular, information from the LTN-51, including ground speed, heading, and drift, are updated every 1.8 seconds. This is convoluted with the 1 second LTN buffer update rate which creates at least a 0.5 second uncertainty in what time the measurements were taken. At the 15 rps scan rate 27 ± 7.5 scans will occur between updates of these critical motion parameters.

The equations employed to systematically correct the geometry of the NS001 data are given in Table 5. Note that since the NS001 instrument is roll-compensated this parameter is not included in the equations. Clock time recorded in the NERDAS and NS001 data are used to register the data sets. The LTN-51 derived parameters are cubicly interpolated and linearly smoothed to reduce the discontinuous nature of the observations. Bad NERDAS records, as noted in the JSC NERDAS data quality report, are replaced with interpolated values.

Preliminary experiments employing the NERDAS data to systematically correct the NS001 image geometry have been dissappointing. The resultant image for the 8/30/79 data is shown in Figure 14. Analysis of this image compared to ground conditions indicates that the technique and/or NERDAS data do not properly account for aircraft variations in drift and/or ground speed. Although the LTN-51 data appear suspect, numerous factors, such as the

TABLE 5

SYSTEMATIC GEOMETRIC CORRECTION
USING NERDAS DATA

FOR ROLL COMPENSATED SCAN MIRROR VELOCITY

$$X = X_o + h \tan\theta \sin\phi - h(\tan\psi/\cos\theta)\cos\phi$$

$$Y = Y_o - h \tan\theta \cos\phi - h(\tan\psi/\cos\theta)\sin\phi$$

$$X_o(t+\Delta t) = X_o(t) + \int_t^{t+\Delta t} v \sin(\phi+\delta)\,dt$$

$$Y_o(t+\Delta t) = Y_o(t) - \int_t^{t+\Delta t} v \cos(\phi+\delta)\,dt$$

where: X_o, Y_o = nadir coordinates
Δt = scan period
θ = pitch
ϕ = heading
δ = drift
ψ = scan angle
h = altitude
v = ground speed
f = frequency of observation

UPDATING X_o, Y_o WITH NAVIGATION DATA (NERDAS)

(1) Find nearest observation times from NERDAS

$t_i \le t \le t_{i+1}$ where: $i = \mathrm{INT}\{(t-t_o)/f+1\}$

(2) Obtain values for each scan by cubic interpolation

$$Z(t) = \sum_{n=0}^{3} a_n t^n$$

where: Z represents $[\theta, \phi, \delta, \psi, h, \text{ or } v]$
using NERDAS values for $Z(t_k)$ $i-1 \le k \le i+2$
solve for a_n $n = 0, \ldots 4$

(3) Calculate nadir displacement between scans assuming

$$\int_t^{t+\Delta t} Z\,dt = \sum_{n=1}^{4} \frac{a_{n-1}}{n}\left[(t+1/f)^n - t^n\right]$$

where: Z represents $v \sin(\phi+\delta)$ or $-v \cos(\phi+\delta)$

and a_n is determined by technique used in step (2)

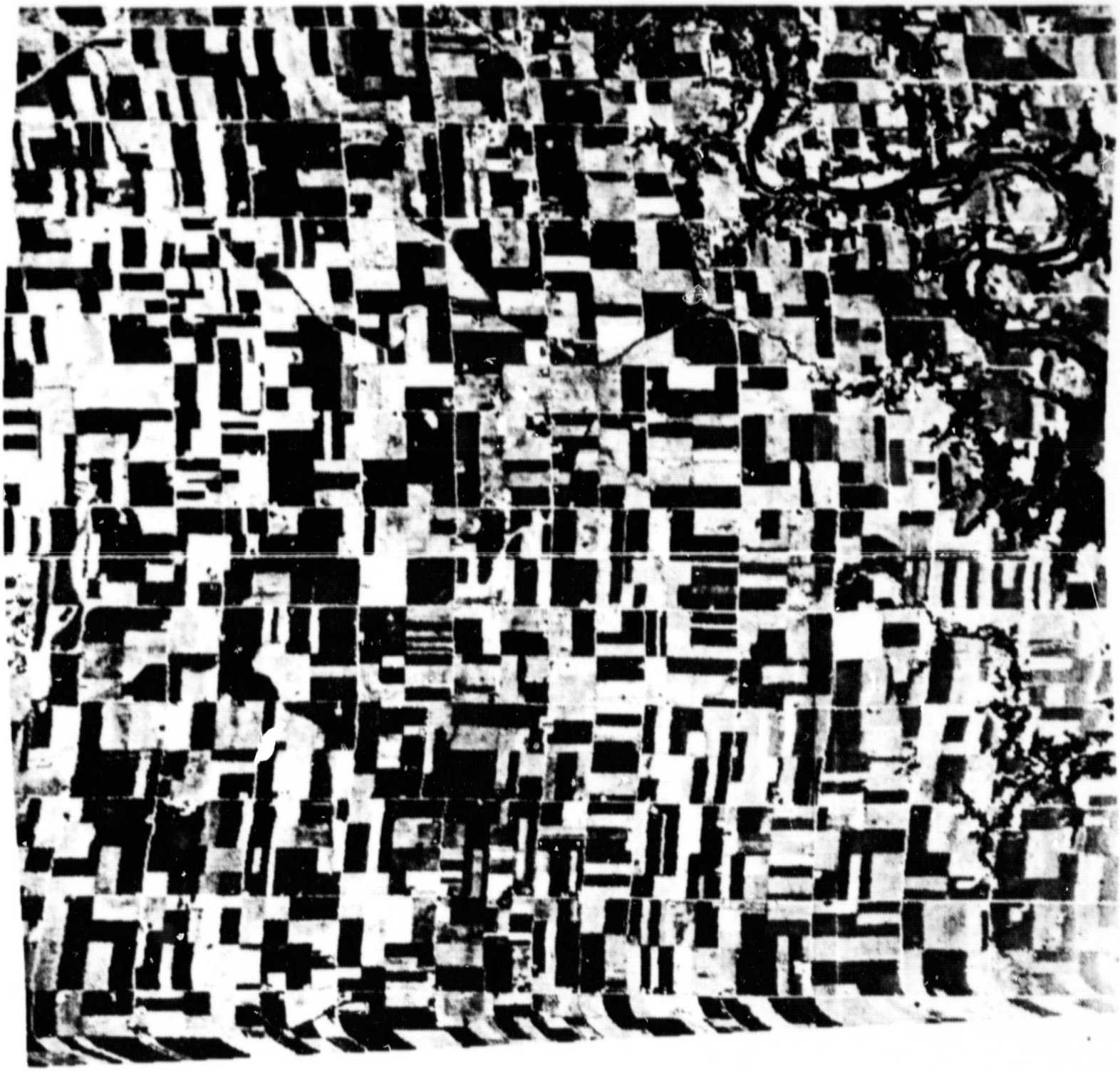

Figure 14

8/30/79 NS001 Data Systematically
Corrected Using NERDAS Data

alignment between the NS001 and the various motion detectors or innaccurate treatment of velocity effects are other possible sources of error.

Further analysis of these problems is required. the systematic approach to geometric correction is the best general solution to rectification of aircraft scanner imagery. The Columbia/GISS staff will explore a number of alternatives during 1982. One approach to resolving the current discrepancies in the systematic technique will be to examine how well that data can be brought into accord with the control points by varying the magnitude of individual aircraft motion parameters.

TM Simulation

Once the ground resolution, radiometry, and geometry of the NS001 data are processed a simulation of TM observations may be constructed. NS001 band 5 is deleted from the data and the remaining bands, with the exception of NS001 band 8, are aggregated to the TM 30 meter ground resolution. NS001 band 8 (10.4 - 12.5 μm) is aggregated to 120 meters to simulate the TM thermal infrared band ground resolution. On the basis of the TM orbital parameters the data array is rotated and an array of 366 by 318 pixels , representing the 5 by 6 nautical mile area of the AgRISTARS supersite, is extracted from the data (Figure 15). The data are then convoluted with appropriate header information, in JSC Universal format, and forwarded to AgRISTARS scientists in Houston as well as subjected to analysis at GISS.

Further steps in processing are possible but have not been carried out in 1981. Examples include calibration of the NS001 data to bidirectional reflectance factor by regression to the FSS data; conversion to nominal radiance and inclusion of expected atmospheric attenuation at satillite altitude; and inclusion of the TM engineering instrument parameters. These additional data processing steps will increase the realism of the simulation

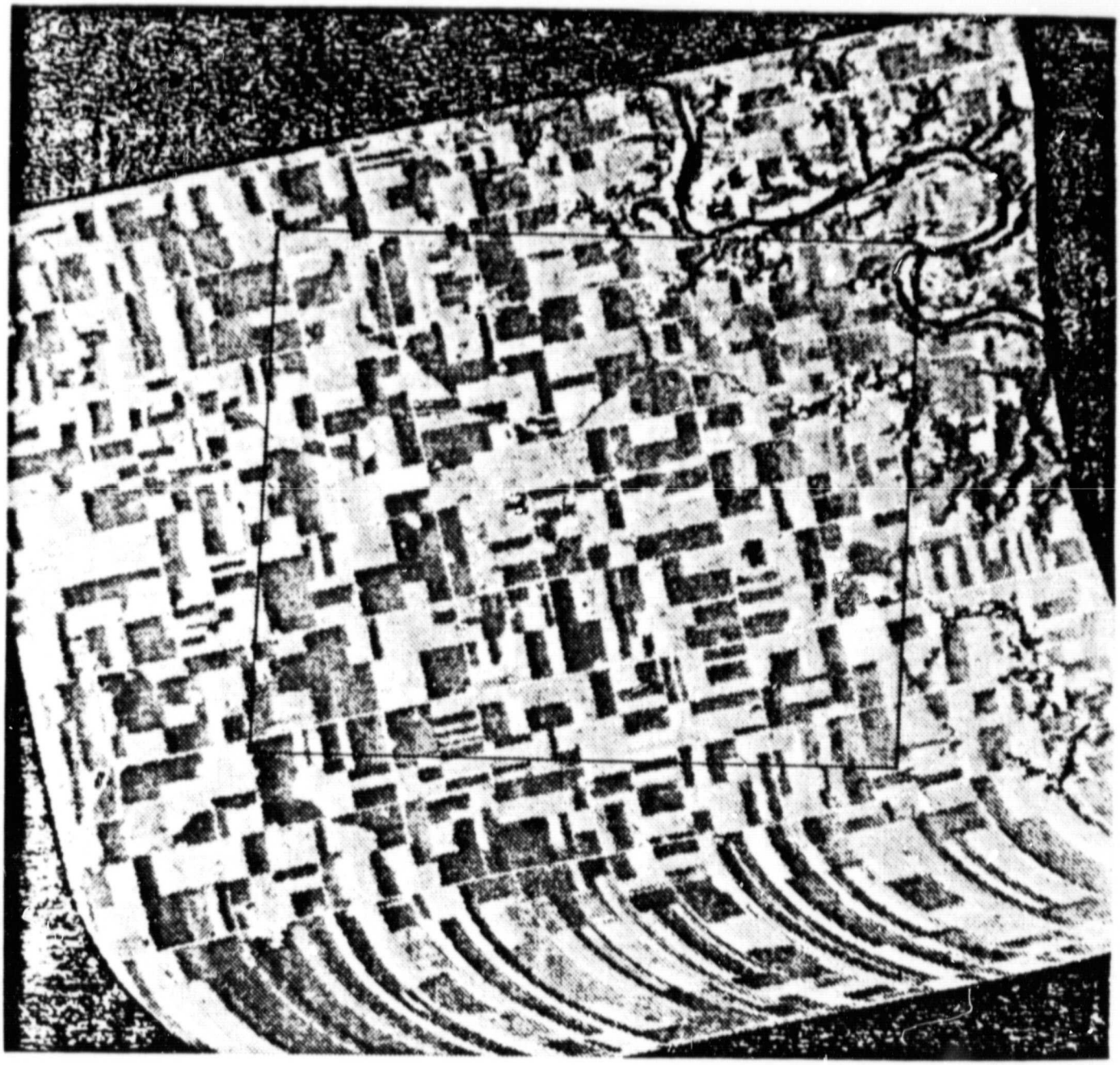

FIGURE 15

ROTATED, TM RESOLUTION

of the expected satellite TM observations. Further progress in this area is expected in 1982.

Simulation of TM Observations from FSS Data

The Field Spectrometer System (FSS), a high spectral resolution (0.02 μm, 0.4-1.1 μm; 0.05 μm for 1.1-2.4 μm; 0.5 μm, 8.0 -14.0 μm) nonimaging instrument, periodically observes the AgRISTARS supersites from a helicopter platform at a nominal altitude of 60 meters. Missions are typically flown on a 9 to 18 day cycle during the growing season, in phase, as much as possible, with Landsat observations of these locations. A set of 10 flightlines are flown during each observation period. The flightlines are planned to pass over 80 fields that are also periodically observed by USDA field enumerators. Instrument calibration is achieved by observing a panel of known reflectance before and after each pair of adjacent flightlines are completed. A boresighted 70 mm camera is operated in conjunction with the FSS instrument to provide a visual assessment of the ground conditions being observed by the spectrometer.

The FSS data are preprocessed at the Johnson Space Center to selectively extract only observations of the 80 periodically observed fields and the calibration panel. These data are forwarded to LARS-Purdue University, where the data are converted to bidirectional reflectance factor by calibration to the panel observations. In addition, the field enumerator observations are appended to the appropriate FSS observations. The FSS instrument generally acquires multiple observations of each field (the number depends on the field dimension in the flight direction). Both single-scan and field average data are produced by the LARS staff. LARS processing of the field average data includes a statistical method to delete "unlike" observations prior to computation of the field means (Biehl, 1979).

The Columbia/GISS staff acquire the processed FSS data from LARS and carry out further data processing to simulate TM, Landsat and other sensor systems spectral configuration. The nominal spectral configuration of the FSS instrument is 0.02 μm between 0.4 -1.1 μm and 0.05 μm between 1.1 -2.4 μm. Studies by GISS and LARS scientists suggested the actual configuration deviates from these specifications. A bench test of the FSS filter wheel revealed that the spectral transmission of the filter wheel is a nonlinear function of the filter wheel position (Barrnett, 1980). Based on JSC recommendations, the recalibrated FSS spectral intervals are used at GISS for data processing. TM, Landsat MSS and other spectral reflectances are computed from the FSS data by integration of the appropriate FSS observations weighted by the proportion of solar illumination in each FSS spectral interval. This computation produced the "effective" spectral bidirectional reflectance factor that the TM, Landsat MSS or other instrument would observe. Figure 16 provides an example plot of FSS data and integrated TM band reflectance from Webster County, Iowa AgRISTARS supersite. Additional simulation steps that may be included to produce more realistic results include: conversion to nominal observed radiance, simulation of atmospheric effects observed from satellite altitude, inclusion of appropriate sensor filter functions, and conversion of radiance measurements to count data based on sensor engineering data.

B. Analysis of TM Simulations

One of the major reasons to simulate TM satellite observations is to provide a data base with which to evaluate the potential information content of TM observations for earth resources research. One pressing issue is whether the TM band 5 (1.55 -1.75 μm), mid-infrared (or shortwave infrared) radiance data will provide information about earth resources that current Landsat MSS

ORIGINAL PAGE IS
OF POOR QUALITY

FIGURE 16

SOYBEANS

FIELD 40 PLANTED: 5/14/79

WEBSTER CO., IOWA

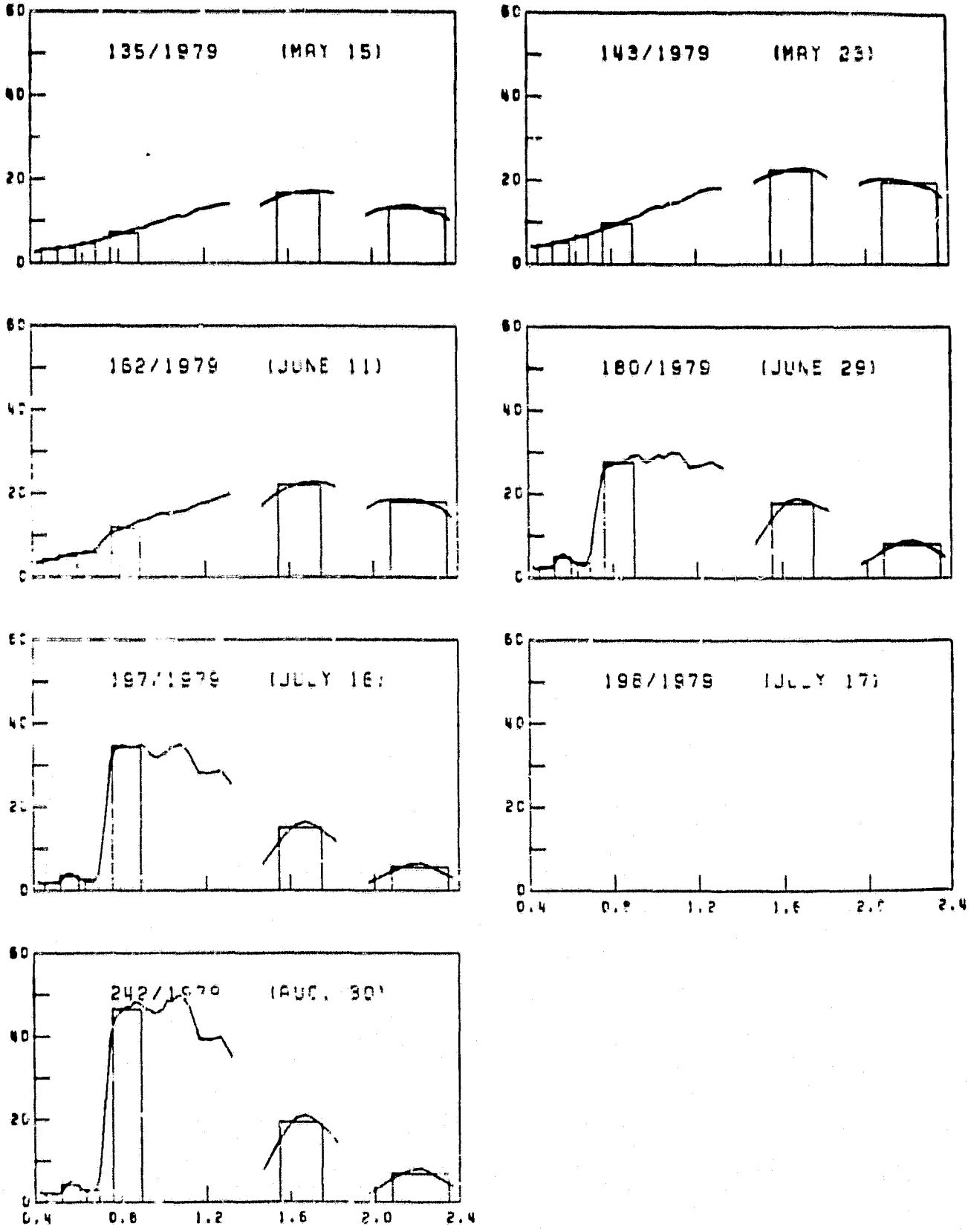

bands do not. This band was selected for observation of vegetated landscapes on the basis that leaf reflectance variations in these wavelengths are principally a function of leaf water content, versus pigments in the visible and leaf mesophyll structure in the near-infrared. However, only limited research has been conducted to access the comparative utility of the 1.55 - 1.75 μm band for vegetation analysis.

In 1981 Columbia/GISS staff conducted a preliminary study of the mid-IR (1.55 -1.75 μm) reflectance behavior of corn and soybeans from the data collected in Webster County,Iowa. The investigation included histogram analysis and parallelapiped classification of the processed NS001 data; a comparative analysis of the NS001 and FSS data for 8/30/79; and temporal analysis using the FSS data. The principal conclusion of this work is that the 1.55 -1.75 μm TM band should improve corn-soybean discrimination in comparison to observations restricted to visible and near-infrared portion of the spectrum. In particular, for these observations of Webster County, Iowa, the 1.55 -1.75 μm measurements provide corn-soybean separability earlier in the season than visible and near-infrared observations.

Experiment Design

NS001 data, FSS data and ground periodic observations collected during 1979 for the Webster County, Iowa AgRISTARS supersite were used for analysis. Eighty fields within the site, selected by the field enumerator prior to the growing season, are observed every 9 to 18 days; as much as possible, in conjunction with other observations by the FSS, NS001, and Landsat sensors. To produce comparative results, the analysis was constrained to those fields which were observed by both the NS001 and FSS instruments and which could be unambigiously located in the NS001 data. Four fields (29, 30, 37 and 79) were not observed by the FSS (apparently due to chickens that were disturbed by the

helicopter) and three fields (8,17, and 22) could not be accurately located in the NS001 data due to ambiguities in the available ancillary information. Of the 73 remaining fields, 36 were corn, 33 were soybeans and 4 were oats.

Analysis of the 8/30/79 NS001 Data

The NS001 data were radiometrically adjusted and resampled to 30 meter ground resolution, as previously described. The 73 fields were located in printer grayscale maps of the data by consultation with AgRISTARS field boundary maps and aerial photography taken during the NS001 overflight and earlier in the 1979 growing season. The analysis was constrained to "field-center" pixels to study the typical reflectance behavior of corn versus soybeans canopies; indepedent of mixed pixels at field borders. Field-center pixels were defined by the largest single rectangle which could be located within the field without including farmsteads, drainage ditches or other non-crop features.

Classification Approach

Visual inspection of the NS001 data on the GISS image display system suggested that corn and soybeans could be more easily discriminated in TM band 5 than in TM bands 2, 3 or 4. To verify this observation, the data were subjected to numerical classification using the GISS-ISURSL parallelapiped classifier (Hyde, Goward and Mausel, 1977) . 10 corn fields, 10 soybeans fields and 1 oats field were randomly selected, on the basis of field number, to serve as test fields. The remaining fields served as training fields. Several band combinations, specifically bands 2 and 3; bands 2, 3, and 4; bands 2, 3 and 6; and bands 2,3,4, and 6, were used to classify the data.

Preliminary class signatures were extracted from the test field data by computing band means and standard deviations for each crop. The parallelapiped class signature was then defined, for each band, as the range of data within two standard deviations from the mean. Class order is a significant component

of the GISS-ISURSL parallelapiped classifier because where class signatures overlap a pixel will be assigned to the first class in which it is a potential member. The strategy employed is to order class signatures within the classifier with respect to signature range magnitude. The class with the smallest signature range is entered first. In this case, the corn signature was the least variable and the oats signature the most variable. The results of training field classification for the preliminary signatures are given in Table 6.

To evaluate the performance of the parallelapiped classifier a proportion estimate is calculated. This proportion compares the actual number of pixels in the class training fields with the numbers of pixels classified as being members of that class. Where the proportion is 100, the classified and actual are the same and the classification is considered accurate. Proportions larger than 100 indicate an overclassification of the category and smaller indicate underclassification. Because the parallelapiped classifier is order dependent the overclassification of the corn for the bands 2 and 3 combination indiacted that the corn signature was too broad and could be impoved by reducing the signature range. This signature refinement is conducted interactively by reducing the upper and lower bounds of each band until the best proportion estimate is achived. Table 7 presents the results of this analysis. Note that a significant improvement is achieved in corn/soybeans classification for the bands 2,3 combination. A minor improvement is achieved for the 2,3,4 combination and no change was necessary in the remaining band combinations.

Classification Results

The test field classification results for the 2,3,5 and 2,3,4,5 TM band combinations are of particular interest. In those cases where the TM 1.55 -

TABLE 6

PARALLELAPIPED CLASSIFICATION OF 8/30/79 NS001
PRELIMINARY SIGNATURE

PERFORMANCE FOR TRAINING FIELDS

CHANNELS	OVERALL	PROPORTION		
		C	S	O
2,3	65.2	180	34	100
2,3,4	97.7	105	96	100
2,3,6	99.8	101	100	100
2,3,4,6	99.8	100	100	100

TABLE 7

PARALLELAPIPED CLASSIFICATION OF 8/30/79 NS001 DATA

PROPORTION ADJUSTED PERFORMANCE FOR TRAINING FIELDS

CHANNELS	OVERALL	PROPORTION		
		C	S	O
2,3	91.0	100	100	100
2,3,4	97.9	99	100	100
2,3,6	99.8	101	100	100
2,3,4,6	99.8	100	100	100

1.75 μm band is included classification accuracy is improved by approximately 2%. This suggests that the mid-infrared band will improve our ability to discriminate corn and soybeans during this period of the growing season. Evaluation of the training field performance statistics confirms this conclusion (Table 8). Classification accuracy is approximately 6% higher with TM band 5 included.

Discussion

Laboratory investigations of corn and soybeans leaf spectra (LARS, 1968) in the 1.55 -1.75 μm spectral range have observed the same differential reflectance behavior that is observed in this classification study of NS001 data. In essence, the reflectance behavior of corn and soybeans leaves differs most sharply in the 1.55 -1.75 um portion of the electromagnetic spectrum. Little is known about how this leaf reflectance behavior translates to canopy reflectance behavior. Examination of histograms of the corn and soybeans data extracted from the NS001 data (Figure 17) suggests that although on average the reflectance difference between corn and soybeans about the same in the near-infrared and mid-infrared that the variability of the reflectance in the mid-infrared is less than in the near-infrared.

Comparison of 8/30/79 FSS and NS001 Data

As previously discussed, the radiometrically adjsuted NS001 data and the FSS data, integrate to TM spectral bands, are highly correlated when field means are compared. Further evidence of their equivalence can be noted by comparing histograms of individual observations from each data set. The regression relation between the NS001 and FSS field means was used to convert the FSS bidirectional reflectance factor data to 8-bit count NS001-like measurements. Using the FSS single-scan data, histograms of corn and soybeans

TABLE 8

PARALLELAPIPED CLASSIFICATION OF 8/30/79 NS001 DATA

PERFORMANCE FOR TEST FIELDS

CHANNELS	OVERALL	PERFORMANCE		
		C	S	O
2,3	84.0	90	111	85
2,3,4	89.9	87	115	61
2,3,6	96.1	96	102	82
2,3,4,6	95.8	96	103	59

FIGURE 17

8/30/79 NS001 CORN/SOYBEANS HISTOGRAMS

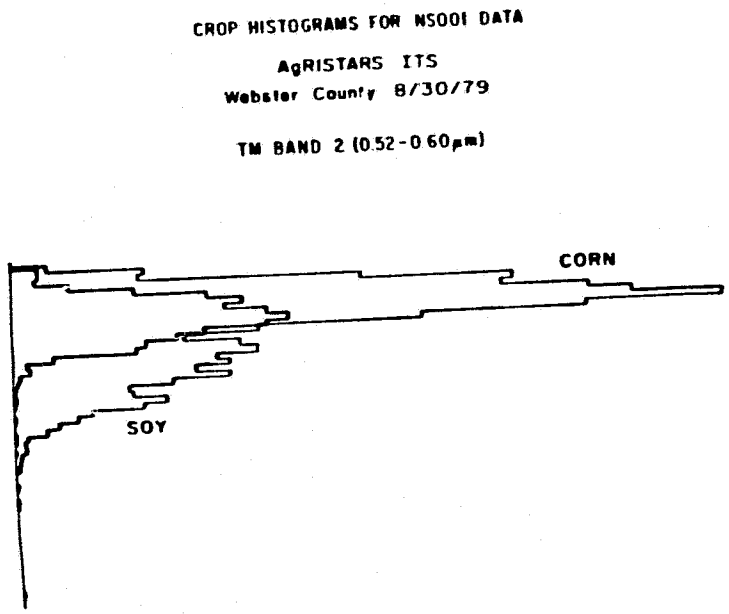

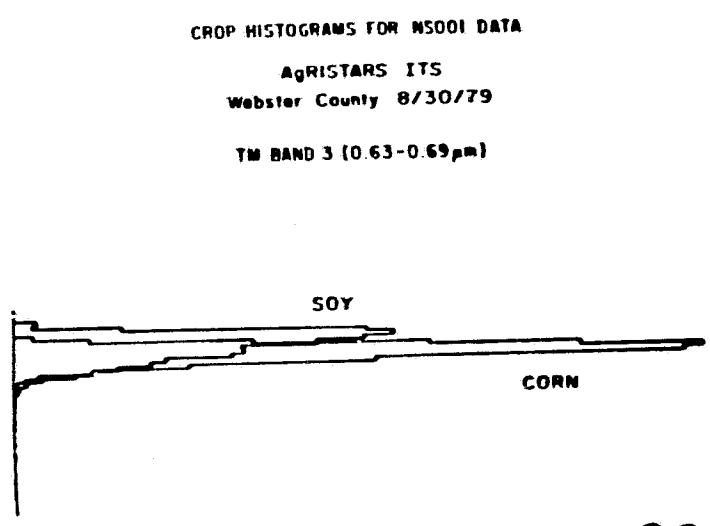

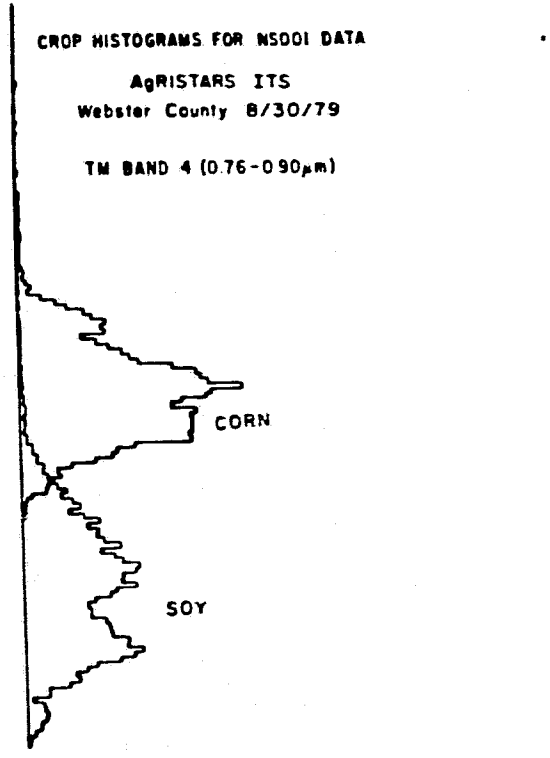

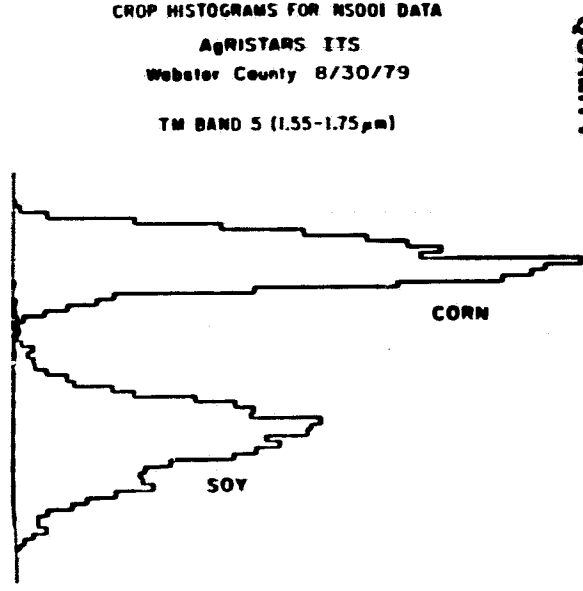

observations were compiled. Because the 8-bit conversion of the FSS data produces highly serrated histograms which disrupts visual inspection, the histograms presented in Figure 18 have been smoothed using a 3 count window moving average.

The FSS histograms in Figure 18 and the NS001 histograms in Figure 17 are quite similar in appearance. The mean and variance behavior of the corn and soybeans canopies display the same patterns in each data set. Note in particular, that the mid-infrared band distribution shows the same comparatively low within-crop variance when compared with the near-infrared band in the FSS data as was noted in the NS001 data.

Temporal Analysis of FSS Data

The comparison of the FSS and NS001 8/30/79 data indicates that they provide common measures of the reflectance behavior of corn and soybeans canopies. The 8/30/79 data suggests that TM mid-IR observations may improve corn/soybeans discrimination on this data. However, analysis of current Landsat data shows that at this time of the growing season, after corn has tasselled, corn and soybeans are not difficult to separate using the visible and near-IR bands.

FSS single scan observations for 6/11, 6/29, 7/16/79 were also processed to construct histograms of the corn and soybeans reflective patterns. Figures 19-22 present the histograms of corn and soybeans FSS observations on these dates and the 8/30/79 observations. Table 9 provides the percent ground cover observed by the field enumerators on these dates.

The histograms reveal a particularly interesting pattern of mid-infrared relectance for corn and soybeans when compared to near-infrared reflectance. On 6/11/79 the FSS observes primarily bare soil and there is little difference in the comparative reflectance of corn and soybean fields in any of the bands.

FIGURE 18

8/30/79 FSS CORN/SOYBEANS HISTOGRAMS

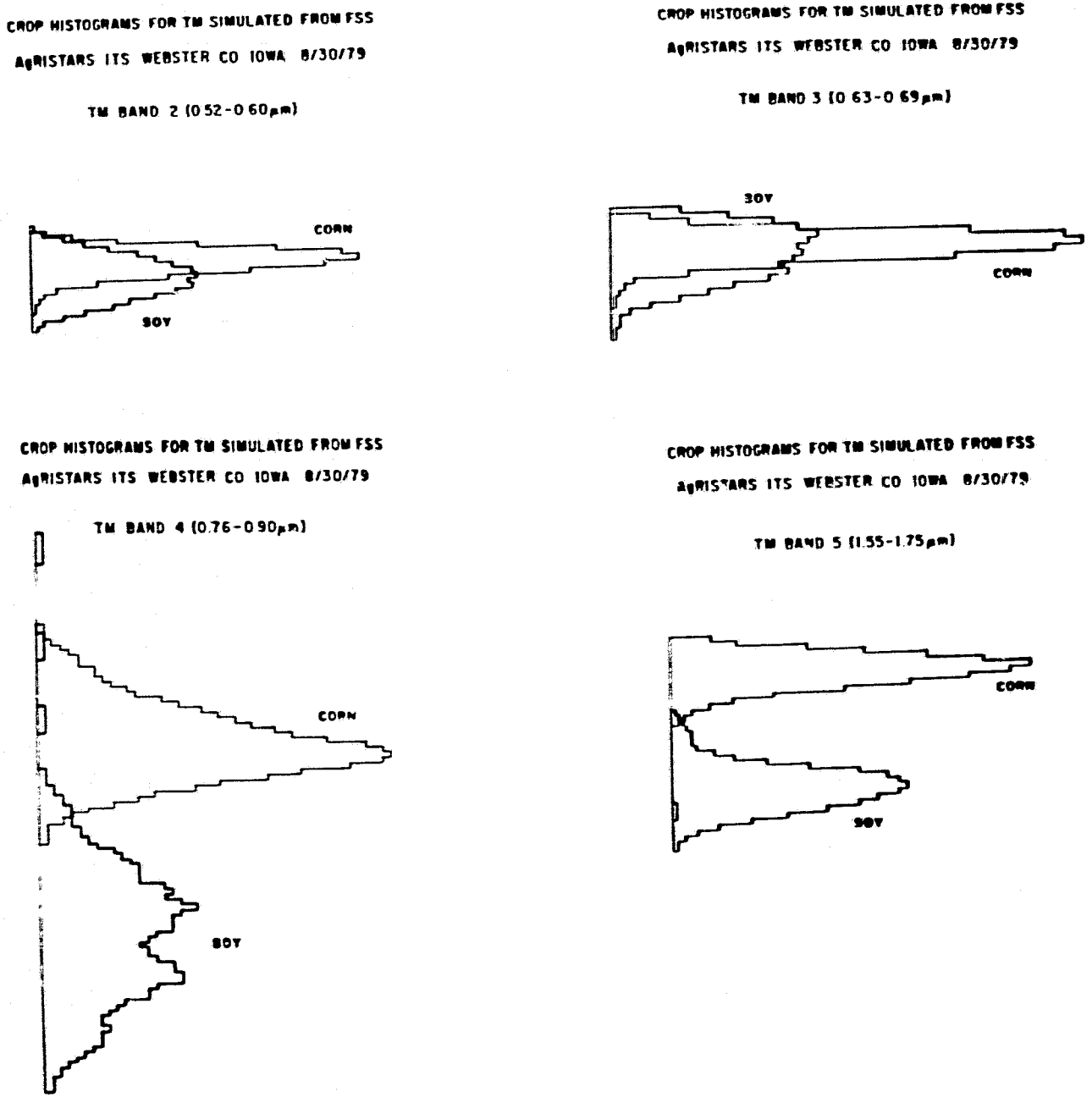

TABLE 9

PERCENT GROUND COVER FOR CORN AND SOYBEAN FIELDS IN 1979

PERCENT COVER	CORN				SOY			
	6/11	6/29	7/16	8/30	6/11	6/29	7/16	8/30
0 - 10	17				30			
11 - 20	21					6		
21 - 30	1	2				7		
31 - 40		6				10	1	
41 - 50		13			2	3	1	
51 - 60		9				1	3	
61 - 70		5				1	6	
71 - 80							12	
81 - 90							7	
91 - 100			36	38			3	33

CROP HISTOGRAMS FOR TM SIMULATED FROM FSS AgRISTARS ITS WEBSTER CO. IOWA 1979 CROPPING SEASON TM BAND 2 (0.52-0.60μm)

CORN —

SOY ----

JUNE 11

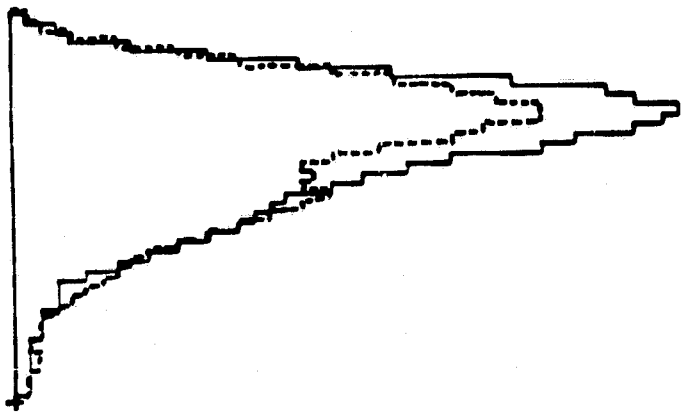

JUNE 29

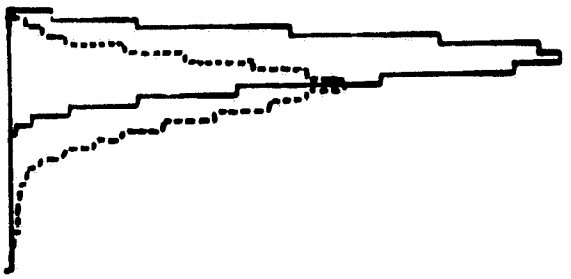

JULY 16

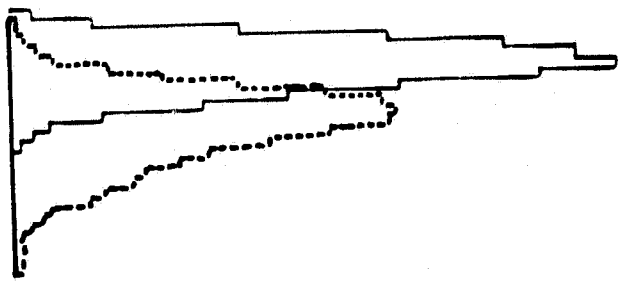

AUGUST 30

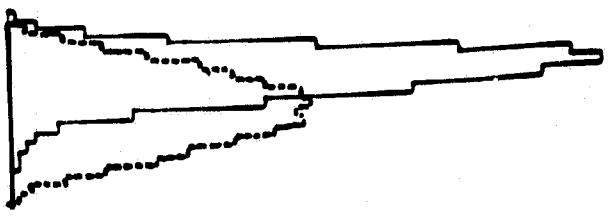

FIGURE 19

CROP HISTOGRAMS FOR TM SIMULATED FROM FSS
AgRISTARS ITS WEBSTER CO. IOWA 1979 CROPPING SEASON
TM BAND 3 (0.63-0.69 μm)

CORN —
SOY ····

JUNE 11

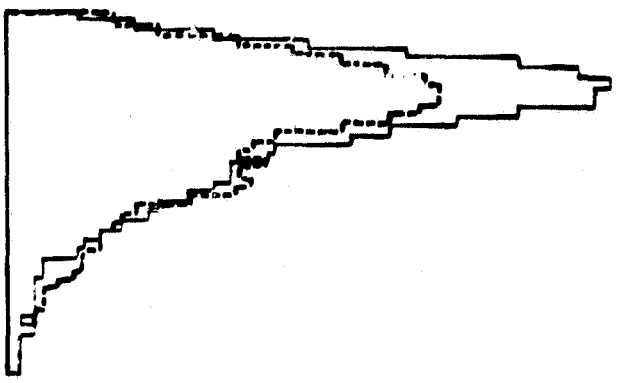

JUNE 29

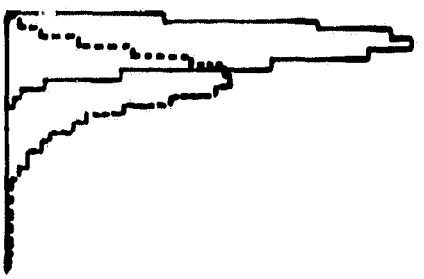

JULY 16

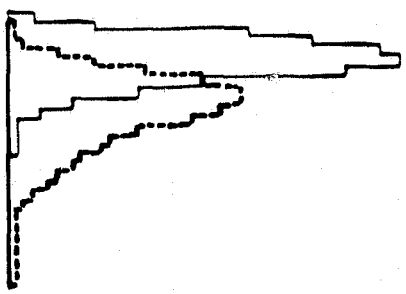

AUGUST 30

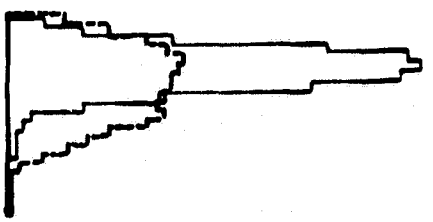

FIGURE 20

CROP HISTOGRAMS FOR TM SIMULATED FROM FSS AgRISTARS ITS WEBSTER CO. IOWA 1979 CROPPING SEASON TM BAND 4 (0.76 - 0.90μm)

CORN ——
SOY ----

JUNE 11

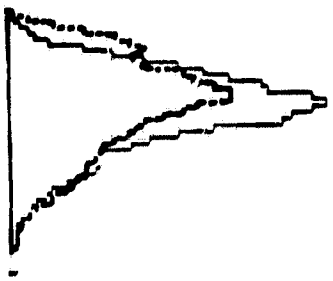

JUNE 29

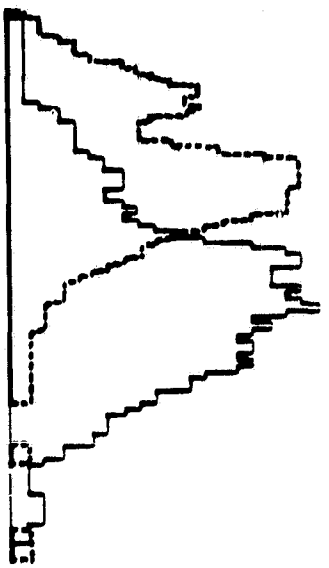

JULY 16

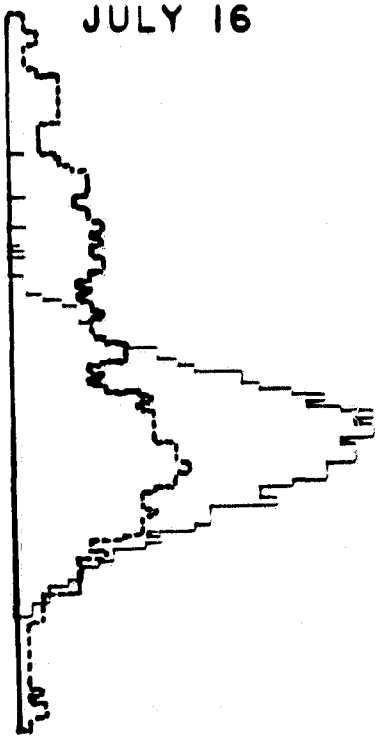

AUGUST 30

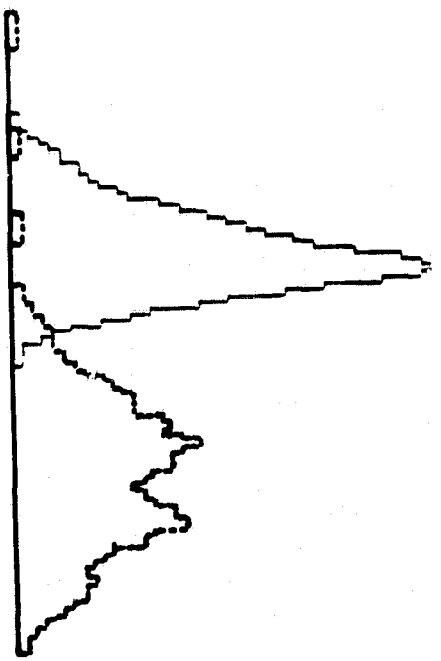

FIGURE 21

CROP HISTOGRAMS FOR TM SIMULATED FROM FSS
AgRISTARS ITS WEBSTER CO. IOWA 1979 CROPPING SEASON
TM BAND 5 (1.55-1.75 μm)

CORN——
SOY----

JUNE 11

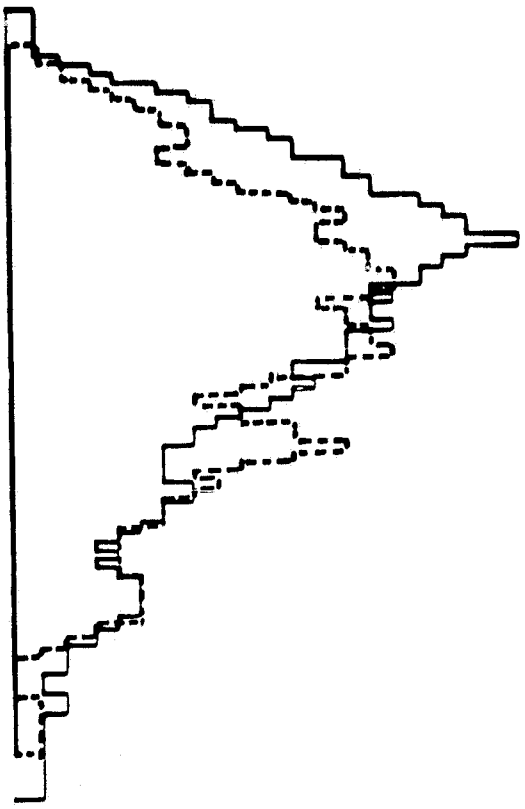

JUNE 29

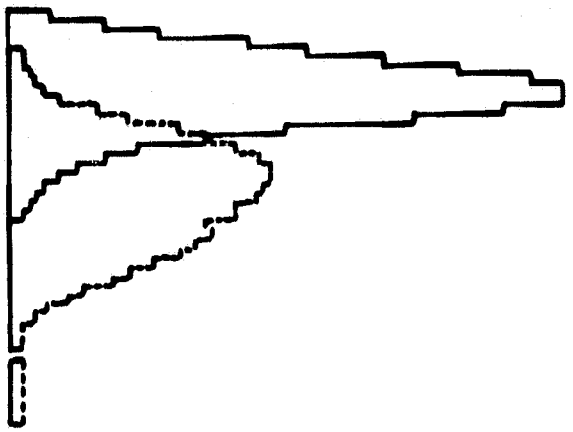

JULY 16

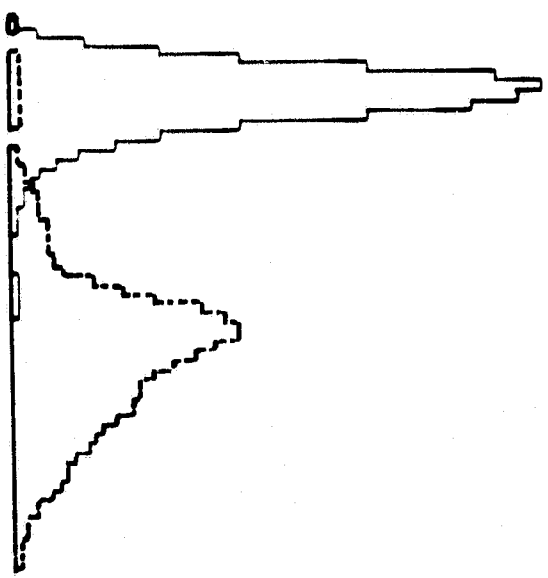

AUGUST 30

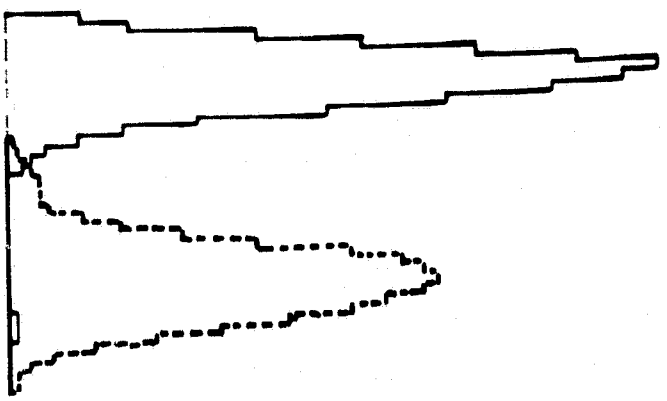

FIGURE 22

Conclusions

The GISS/Columbia Earth Resources group has been intensively involved, during 1981,with activities directed at simulating TM observations and evaluating the potential information content of these observations. The NASA/AgRISTARS field measurements program continues to provide extensive data to conduct this research. The GISS/Columbia staff have developed processing and analysis techniques to utilize this data base. The 1981 research program has successfully addressed several outstanding NASA research objectives concerned with preparation for the analysis of satellite acquired TM observations. The more extensive field observations collected at the AgRISTARS supersites during the 1980 and 1981 growing season present a major analysis challenge. The experience gained by the GISS/ Columbia staff in analysis if the 1979 AgRISTARS data during this year will be invaluable to exploitation of the more recent field measurements and in analysis of the soon-to-be acquired satellite TM observations.

C. Analysis of Snow Cover and Wetlands from Landsat Data

The GISS/Columbia group, in cooperative research program with U.S. Army Corps of Engineers applications scientists at the Cold Regions Research Laboratory, Hanover, New Hampshire, have, during 1981, carried out analysis of selected Landsat scenes. This research objective is to determine the utility of Landsat numerical observations for mapping and analysis of snow cover and wetlands. Michael Miller, a graduate student of the Department of Geography, has served as senior analyst for these activities. Drs. Goward and Ungar of the GISS/Columbia group provide research direction in consultation with CRREL scientists, Carolyn Merry, Dr. Jerry Brown and Dr. Ike McKim. The following reports describe the research activities.

By 6/29/79, corn fields average 50% ground cover and soybeans 35% ground cover. In the mid-infrared corn fields are less reflective than the soybeans fields whereas in the near-IR the reverse is true. On 7/16/79 corn canopies are reported to have 100% ground cover whereas the soybeans fields average 65% but are highly variable. The mid-IR data show that corn is still less relective than soybeans and better separated than on 6/29/79. However, in the near-IR the soybeans reflectance is highly variable and mixed with the corn reflectance. By 8/30/79 both crops are at 100% ground cover and soybeans are more reflective than corn in both TM bands. These histograms suggest that the TM mid-IR observations will significantly improve early season corn/soybeans discrimination when compared to current Landsat observations.

Discussion

This investigation of the mid-IR reflectance behavior of corn and soybeans canopies suggests that TM observation in this wavelength interval will improve both early season and through-the-season discrimination of corn and soybeans. These conclusions are drawn, however, from one growing season in one location. Further analysis of observational data will be required to establish the general applicability of these findings.

In depth evaluation of these results will require examination of the physical processes that lead to differential reflectance behavior of corn/soybeans canopies in the mid-IR. Interactions between leaf reflectance properties, canopy architecture and background soil need to be examined. Although further empirical studies may be able to confirm the behavior observed in this study, prediction of where and under what conditions this behavior will be observed will require physical understanding.

Progress Report: Remote Sensing of Snow

Michael S. Miller July - December, 1980

Introduction: Landsat scenes are being investigated in conjunction with ground snow course measurements to determine the utility of the remotely sensed data for snow cover evaluation. Although satellite data have proven useful for estimating areal extent of snow, applicability in forested hydrologic basins, and for other descriptors of snow cover (e.g. depth, water equivalent) are less obvious.

Study Site: Allagash, St. John Rivers confluence area, Maine. Land cover is a mix of deciduous, coniferous, and mixed forests, clearings, agriculture, and water surfaces.

Achievements (July - Dec., 1980)

1. Using a May 31, 1978 Landsat image, the 300×300 pixel study area (153 sq. miles) was classified using the GISS-MAP1 classification routine. Results, in percent cover of the area, are:

Water	2.2%	Mixed Forest	52.3%
Deciduous Forest	16.3%	Clearings	.5%
Coniferous	28.2%	Agriculture	.5%

2. Using these percents as weighting factors for ground snow depth measurements, average snow depths for the study region were determined for four days for which good quality Landsat coverage is available:

February 11, 1978	29.01"
January 11, 1979	23.63"
December 24, 1978	20.94"
January 6, 1978	17.06"

3. Landsat MSS digital data have been investigated to determine whether there is a crrelation between snow depth and the measured intensities in the four spectral bands. All sites were thus evaluated. Band ratios and summations were considered, as was the inclusion of a sun elevation factor to compensate for differences in incoming radiation on different days. In most cases (see Figure one a-d) little correlation between snow depth and Landsat counts/energies was noted.

4. Although radiances measured in reflected visible and near-infrared wavelengths within an individual pixel do not increase (or decrease) with increased snow depths beyond several inches, it is believed that the regional landscape does change. In the northeast forests, the vegetation canopy is not uniform. Mixtures of clearings and coniferous and deciduous forests at various stages of growth allow upper canopies and understories of differing heights and densities. As snow accumulates, different levels of vegetation would be expected to be covered with snow. Figure two a-d show band 7 grayscales for the 300x300 pixel Allagash area for four days. As is seen, increasing snow depth results in increasing 'whiteness' of the area.

5. Histograms of the energies have been investigated to quantify this change (figure 3 a. A 'no snow' scene in autumn shows a band 7 histogram that is unimodal and of low variance (3-a). As snow depth increases (3-b to 3-e), there is a decreasing in peakedness and increasing of skewness toward the bright end of the distribution. This indicates

that as snow depth in a diverse land cover increases, increasingly more pixels will become 'snow pixels', migrating in the regional histogram from the apparantly snowless vegetation peak to the brighter (snow) intensities.

Projected work (Jan. - June 1981)

Examination of gray scales and histograms for additional snow scenes of the Allagash/St. John area will continue. This is to dtermine the validity of the preliminary observations.

In addition, gray scales will be examined in conjunction with the derived classification map to determine which vegetation types contribute to increased brightness as snow depth increases.

Similar examination will be initiated in the Danville, Vermont area in the Sleepers River Basin. Records of snow depth for a variety of land cover types are available for this intensively monitored basin in northeastern Vermont.

Problems encountered to date: The major obstacle to this research into snow cover is the low number of available Landsat scenes for this region during snow seasons. This is due primarily to the satellite's cycle and to the frequency of cloud cover, particularly in the important snow melt period.

Figure one. Snow Course and Landsat MSS data for four sites.

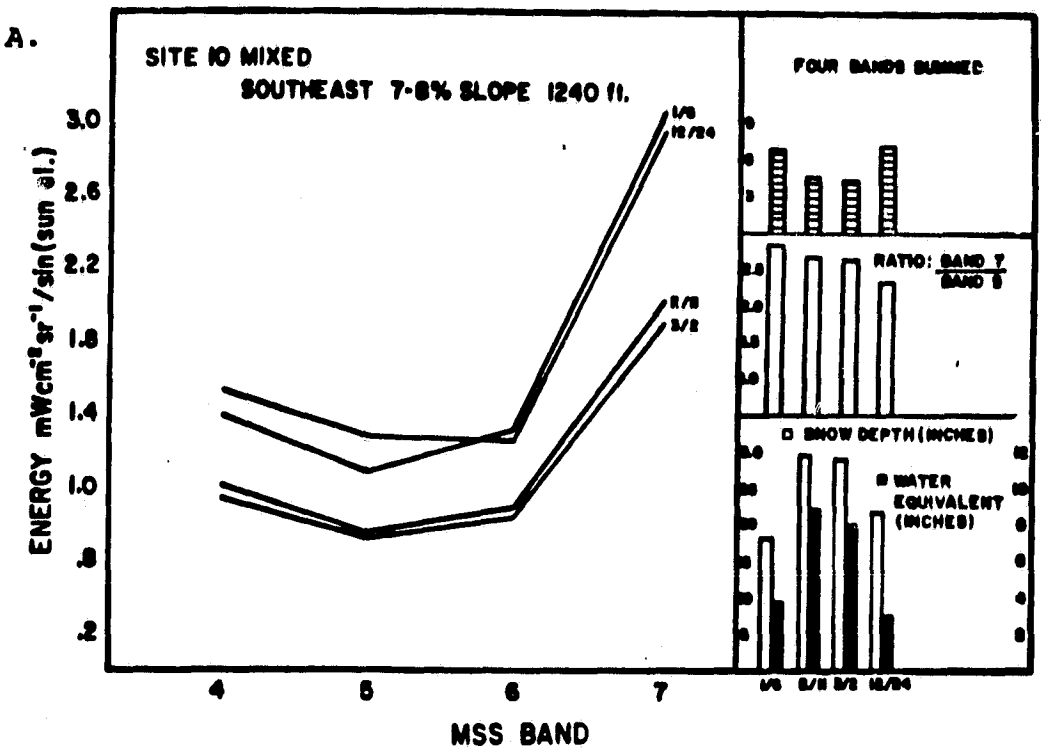

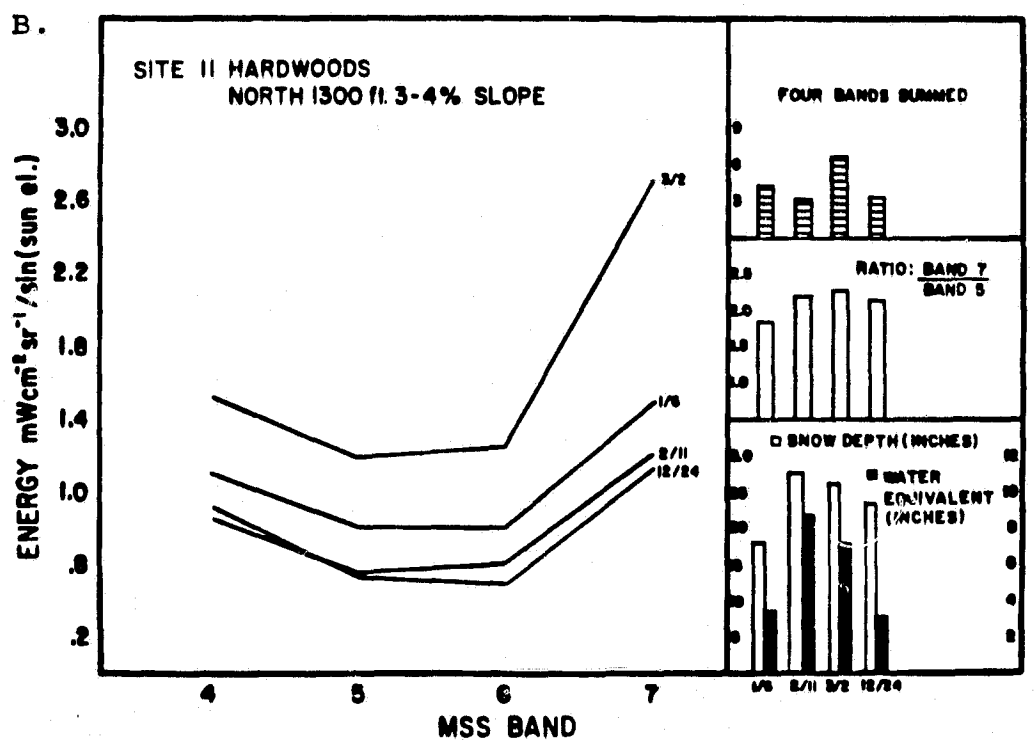

Figure one, continued.

C.

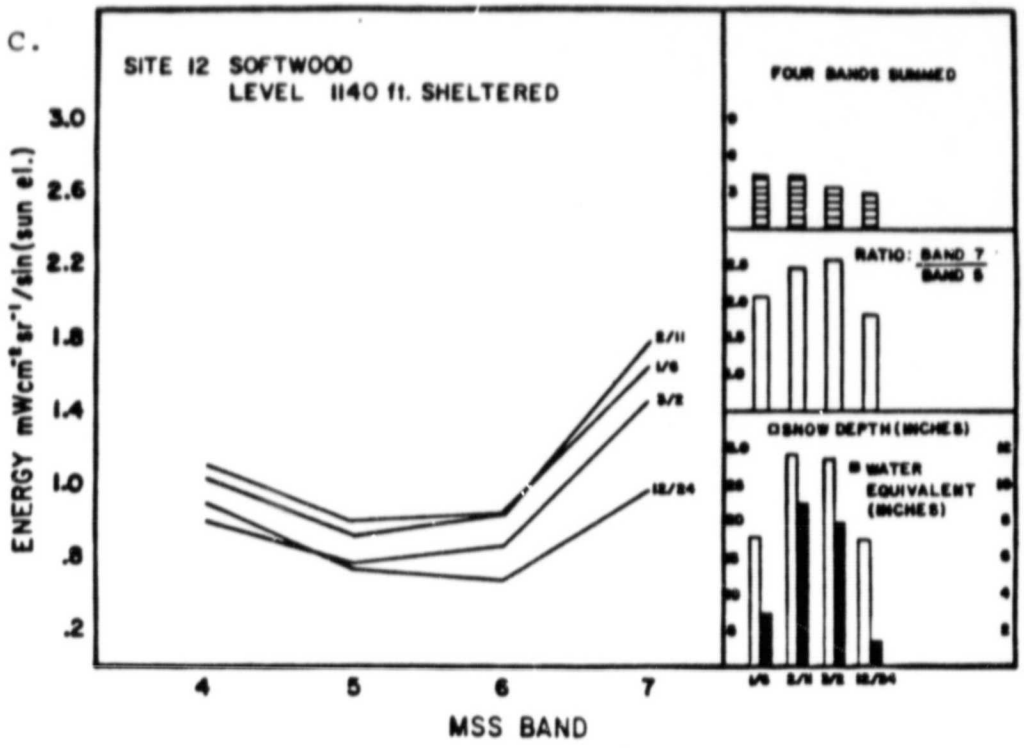

D.

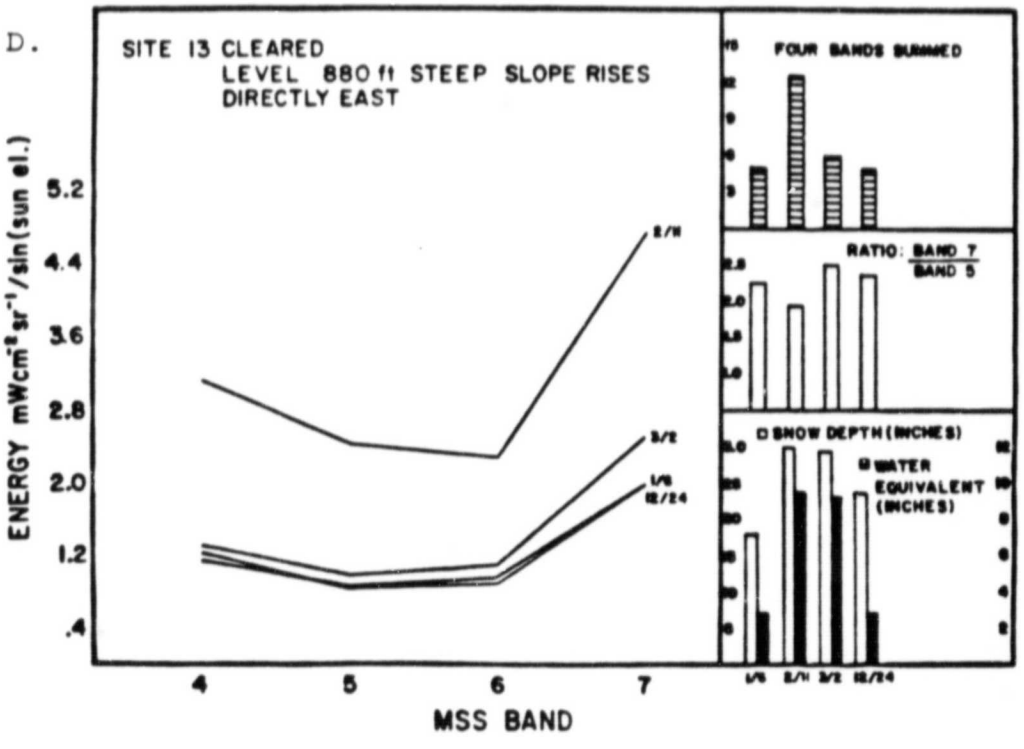

Figure two, continued.

C. January 11, 1979

Average snow depth: 23.63"

D. February 11, 1978

Average snow depth: 29.01"

Figure two. Landsat MSS

Band 7, gray scales.

A. January 6, 1978

Average snow depth: 17.06"

B. December 24, 1978

Average snow depth: 20.94"

Figure Three.

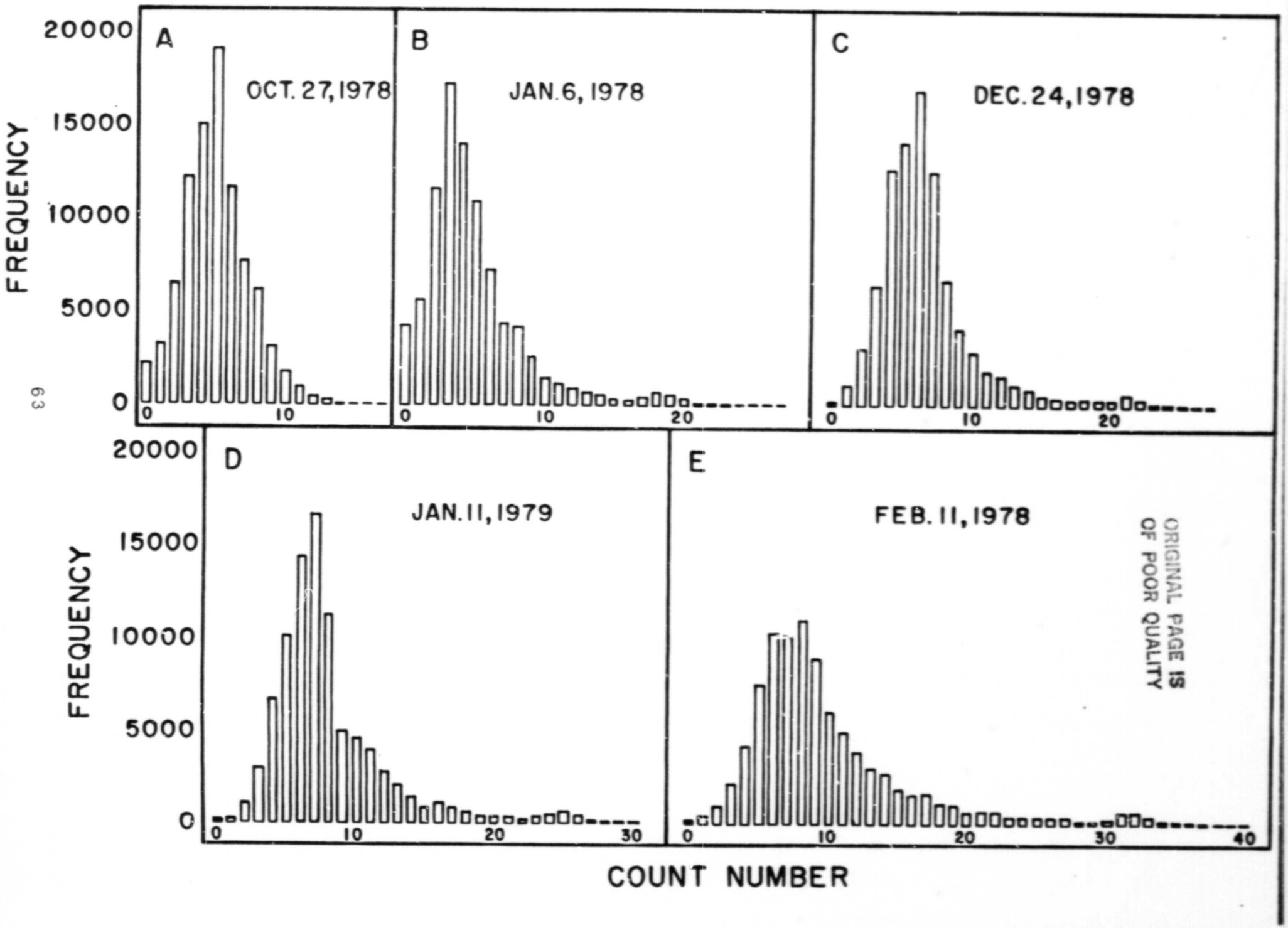

USE OF LANDSAT DIGITAL DATA IN SNOW COVER MAPPING FOR THE UPPER SAINT JOHN RIVER BASIN, MAINE

Carolyn J. Merry
U.S. Army Cold Regions Research and Engineering Laboratory
72 Lyme Road
Hanover, New Hampshire 03755

Michael Miller
NASA Goddard Institute for Space Studies
2880 Broadway
New York, New York 10025

ABSTRACT

Each spring the SSARR (Streamflow Synthesis and Reservoir Regulation) model is used in the Upper Saint John River Basin, Maine, to forecast runoff due to snowmelt and precipitation. One of the main inputs to the model is the extent and distribution of the snowpack. Using point snow course measurements to determine the extent and distribution of the snowpack is a commonly recognized problem. A technique for using Landsat digital data to map the distribution of snow cover/land use categories has been evaluated for use in the SSARR model to improve the accuracy of spring runoff predictions.

Landsat MSS digital data has been investigated to determine whether there is a correlation between snow depth and the measured intensities in the four spectral bands. Band ratios and summations of the four bands were considered, as was the inclusion of a sun elevation factor to account for differences in incoming radiation on different days. A direct correlation between snow depth and Landsat counts/energies does not occur.

Although the Landsat radiances measured in the reflected visible and near infrared wavelengths for a single pixel do not increase (or decrease) uniformly with increased snow depth beyond several inches, it is believed that Landsat radiance values on a regional scale do change. Histograms of the Landsat radiance values for a 300 x 300 pixel (153 sq. mi.) study area have been investigated to quantify the change. A histogram for a no snow scene in the late autumn (27 October 1978) exhibits a unimodal distribution with low variance. As the snow depth increases over the total landscape, there is a decrease in peakedness and a corresponding increase of skewness toward the bright end of the Landsat distribution of radiance. This fact indicates that as snow depth in a landscape increases, additional pixels become 'snow pixels', migrating in the regional histogram from the apparently snowless vegetation peak to the brighter 'snow' intensities.

Various indices of skewness and peakedness (kurtosis) have been examined to quantify the above observation. An index of potential use is defined as:

$$I_s = a_3 * \frac{pop(total)}{pop(mode)} * \cos(\quad) \varepsilon$$

in which I_s is the index of snowness, a_3 is the moment coeffient of skewness, pop (mode) is the pixel population of the histogram mode, pop (total) is the total pixel population and COS(θ) is the cosine of the solar zenith angle. Through linear regression techniques, it was determined for the 300 x 300 pixel Landsat area that:

$$\text{Snow Depth} = 2.079*(I_s) - 1.111$$

in which snow depth is measured in inches. The index of snowness, I_s, was found to predict mean snow depth with a standard error of estimate of $\pm$ 4.2 inches at a 95% confidence level. For different mixtures of canopy cover, the slope and y-intercept would vary.

As a preliminary test of this index of snowness, two winter Landsat passes from previous years were examined for the Allagash - St. John region. Using the index and equation of regression, mean snow depth for February 11, 1973 and April 19, 1974 were estimated at, respectively, 35.49" and 15.89", ±4.44". During those years, ground snow course measurements were not available for the Allagash stations. Closest measurements were taken at Connors, New Brunswick, 12 miles east on the St. John River. Snow depths at Connors were:

February 1, 1973	33.3"
February 19, 1973	37.9"
April 16, 1974	23.7"
May 7, 1974	11.3"

II. Bibliographic search for literature concerning the remote sensing of snow pack characteristics has continued during the report period.

III. Visit was made on March 25 to the Sleeper's River Research Watershed. Snow courses, meteorological stations and streamflow measurement sites were examined in anticipation of studying the land cover - snow pack relationship for this basin in Vermont. Search of Landsat scenes is underway.

PROGRESS REPORT

- Michael S. Miller

Project: Simeon, Nebraska - Wetlands Classification

For Period: September/October, 1980

Objective: To classify Landsat MSS digital data for June 12, 1978 (scene-i.d. 3099-16494) for Simeon (Nebr.) SW and SE Quadrangles. This area lies within the Valentine National Wildlife Refuge. Three cover types are classified: open water, marsh, and subirrigated meadow. Unclassified areas are 'classed' as uplands. This classification is performed for the Waterways Experiment Station, Army Corps of Engineers,

Procedure: 1. The MAP1 classification algorithm developed by Dr. S. Ungar of the NASA Goddard Institute for Space Studies is used in this project. A description of this algorithm is provided in the appendix to this report.

In MAP1, the digitized Landsat counts are converted to energy values (mW cm^{-2} sr^{-1}). For each classified cover type a signature, or group of signatures is required. The area within the Landsat multispectral space surrounding each signature and classified to its cover type is determined by user specified parameters: Δ_{MAX} and WBRT (maximum angular delta, and brightness weighting).

2. Signatures were selected by the evaluation of test sites

within the larger study area. Six to eight test sites were selected from the quadrangles for each of the three cover types. This was accomplished by using the wetlands map overlay (scale 1:24,000) provided by the Omaha District, Corps of Engineers. The overlay was superimposed onto a MSS band 7 grayscale printout. Test sites were delineated for each cover type using the orthophotoquad for reference. The test sites ranged from 5 hectares (12 acres) to 40 hectares (100 acres). To maximize 'purity' of cover type, the sites were selected from the interior of larger homogeneous areas.

3. Unsupervised classifications were run to distinguish distinct classes within each test site. Printouts of the Landsat energies were used to derive signatures for each class. From the unsupervised classifications it was determined that two signatures were necessary to most accurately describe each of the cover types.

Cover Type		Signature (in energy: mW cm^{-2} sr^{-1})			
		Band 4	Band 5	Band 6	Band 7
1. Water	(a)	.29	.15	.08	.09
	(b)	.42	.25	.20	.21
2. Marsh	(a)	.41	.26	.37	1.17
	(b)	.47	.32	.50	1.45
3. Subirrigated Meadow	(a)	.47	.32	.58	1.71
	(b)	.46	.31	.61	1.88

4. The signatures derived in the unsupervised runs were used in the supervised procedure for a larger area approximating the Simeon SW Quadrangle. The supervised classifications were run with a variety of Δ_{MAX} / WBRT combinations, thus altering the set of pixels classed within each cover type. Considerable visual agreement between the classification and wetland map was achieved after fifteen runs. Refinements in agreement resulted after ten additional runs in which signatures were adjusted and rearrangements made in the order in which the signatures were assessed for each pixel (Note: order is of importance in MAP1, as the algorithm is deterministic rather than probablistic). It was found possible to eliminate the need for one of the water signatures without a reduction in classification accuracy.

5. In conversation (mid-September) with Horton Struve of the Waterways Experiment Station, it was decided to extend the classification to include the Simeon SE Quadrangle. Land cover within the two Quadrangles is very similar. Nevertheless, several additional runs were required to take into account some spectral variations across the region.

6. Final signatures, in order of their evaluation within MAP1 are:

Cover Type	Signature				MAX	WBRT
	4	5	6	7		
1. Marsh	.47	.32	.50	1.38	.041	.1
2. Sub. Meadow	.47	.32	.58	1.71	.08	.1
3. Water	.42	.25	.20	.21	.52	.4
4. Sub. Meadow	.40	.30	.58	1.80	.12	.1
5. Marsh	.40	.32	.30	.88	.12	.1

7. Percent cover was evaluated for each of the following classes: open water, wetlands (marsh + subirrigated meadow), and uplands for the entire Simeon SE, SW area. In the table below, these are compared to the corresponding figures for the Simeon SW area used at the Waterways Experiment Station for a ground truth standard. Comparable figures for the entire area were not available.

Cover Type	Ground-Truth	MSS	Difference
Water	8.8%	8.0%	.8
Wetland	35.7%	32.6%	3.1
Marsh		4.6%	
Subirrigated Meadow		28.0%	
Upland	55.5%	59.4%	3.9

8. A tape of the digitized final classification is being prepared for Horton Struve, Waterways Experiment Station.

Appendix

The following description of the GISS MAP1 classification algorithm is taken from:

Merry, C.J. et al., Preliminary analysis of water equivalent/snow characteristics using Landsat digital processing techniques, 1977, Cold Regions Research and Engineering Laboratory, Hanover, NH.

The LANDSAT MSS observation may be thought of as a point in a four-dimensional "color" space, where the values along each axis represent the radiant energy received by the satellite in one of the four bands (this is illustrated for three bands in Fig. 2a). Observations lying in a similar direction from the origin in this four-dimensional color space

are said to be similar in color regardless of their total radiant energy. The distance of an observation from the origin is a measure of the total radiance associated with that data point. The algorithm is primarily designed to combine observations similar in color into the same classification category. There is provision for evaluating brightness differences and for weighting these differences in with the color discrimination when constructing the classification categories.

Discrimination based solely on color is obtained when one examines the difference in direction between the color vectors (observations). If the angle between the observations is smaller than some user-defined *criterion* the vectors are considered to be lying in the same direction and, therefore, the observations are placed in the same category.

There are two modes in which this classification scheme may be employed, supervised and unsupervised. In the supervised mode the user specifies a *signature* (the energy distribution in the four LANDSAT bands). If an observation lies within an angle smaller than the user-defined criterion, δ_{max}, it is said to belong to the category represented by the signature (Fig. 2b). Therefore, all vectors lying within a cone of angle, δ_{max}, about the signature representing category X belong to category X.

In the unsupervised mode the color vector corresponding to the first observation is compared with all subsequent observations. If color vector 1 is similar in direction to color vector 2 (i.e. $\delta\theta \leq \delta_{max}$), observation 2 is placed in the same category as the first observation (Fig. 2c). In a similar fashion observations subsequent to observation 2 are compared to the second observation and so on right up to the last observation. If in the process of constructing categories, a member is found which belongs to a previous category, the new category is *chained* to the original classification category forming one joint category. In effect the unsupervised classification will form several categories based on a criterion specifying maximum color difference permissible between members of the same category.

In addition to discrimination based solely on color, the GISS algorithm provides the capability of weighting total radiance (*albedo*) differences into the discriminant. The percent albedo difference between two observations is computed. This normalized albedo difference is then combined with the color difference angle (expressed in radians) by performing a weighted average in the RMS (root mean square) sense. This albedo-weighted quantity is now compared with the user-defined criterion. A relatively small albedo weighting allows very large albedo differences to disqualify observations that are similar in color from membership in the same category, thereby adding a second level of discrimination.

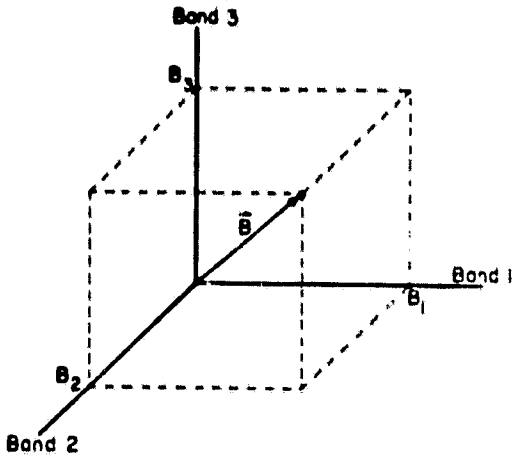

B_i = Energy in Band i

$B_{Total} = \sum_{i=1}^{4} B_i$ = Total Radiance

a. A color vector which is illustrated for three bands.

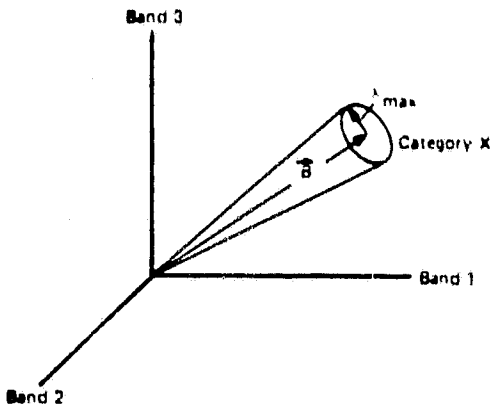

b. Supervised mode. The user-defined criterion, δ_{max}, defines category X about the specified signature, $\vec{B}$. Any color vector that lies within this cone belongs to category X.

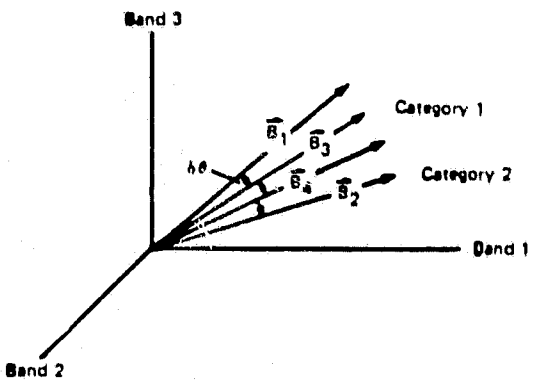

c. Unsupervised mode. $\vec{B}_3$ is similar in direction to $\vec{B}_1$ ($\delta\theta \leq \delta_{max}$) and placed in category 1. $\vec{B}_4$ is similar in direction to $\vec{B}_2$ and placed in category 2. However, $\vec{B}_4$ is also similar in direction to $\vec{B}_3$ (category 1). Therefore, category 1 is merged with category 2.

Figure 2. Concept of the four-dimensional "color" space, represented in three bands.

Project: Burlington, Vermont Quadrangle: Wetland Mapping

Objective: To map potential and definite wetlands; evaluate seasonal images.

Procedure: Two Landsat images of the Burlington area were classified using the GISS MAP1 classification package The dates of the two passes were 13 April 1977 (SCNID 20812-14372) and 26 June 1975 (SCNID 5068-14433).

The first stage in the classification of the two dates was the development of a standard routine for mapping potential wetlands. Potential wetlands are here defined as that set of pixels in the scene which include all wetlands. That is, errors of omission are minimized. However, there may be large errors of comission. The second stage was to perform a second classification on these potential wetlands in which only definite areas of wetlands are identified; errors of comission are minimized. In this second stage, areas of open water, emergent vegetation, and forest/shrub-scrub wetlands were segregated. The two classifications used in conjunction may give a good indication on the locations of the wetlands.

13 April 1977

1) After examining numerous classification possibilities for potential wetlands, the approach finally selected was a one signature, two-band classification using MSS-4 and -5. In the unsupervised mode of MAP1, pixels corresponding to open water were found to cluster around a signature of 0.44, 0.25, 0.00, 0.00 when weighting of bands equalled 1.0, 1.0, 0.0, 0.0. This signature was then applied to the supervised mode with a range of increasing delmax values. The final namelist parameters selected

for this classification were SIG = 0.44, 0.225, 0.00, 0.00; DELMAX = 0.215; WBRT = 0.5; WBND = 1.0, 1.0, 0.0, 0.0.

2) To classify definite wetlands three classes were used: open water, emergent vegetation and forest/shrub-scrub wetlands. All areas identified as potential wetlands in step 1 were classified using a one-band (MSS-7) classification. The namelist parameters used were: a) water: SIG = 0.00, 0.00, 0.00, 0.17; DELMAX = 0.7; WBRT = 1.0; WBND = 0.0, 0.0, 0.0, 1.0; b) emergents: SIG = 0.00, 0.00, 0.00, 0.53; DELMAX = 0.25; WBRT = 1.0; WBND = 0.0, 0.0, 0.0, 1.0; c) forest-shrub-scrub: SIG = 0.00, 0.00, 0.00, 0.55; DELMAX = 0.444.

26 June 1975

3) Using the same procedure as in (1), MSS-4, -5 signature of water (0.40, 0.15, 0.00, 0.00) was applied in the supervised mode with DELMAX = 0.3, WBRT = 0.5, and WBND = 1.0, 1.0, 0.0, 0.0.

4) The nature of the landscape in June made it possible to successfully classify only open water of the three wetland classes. In these cases a four-band classification most accurately identified water: SIG = 0.40, 0.15, 0.10, 0.11; DELMAX = 0.4; WBRT = 0.1; WBND = 1.0, 1.0, 1.0, 1.0.

Comments

1) Seasonal variations are highlighted here. Spring images are best for identifying wetlands in the Northeast - water table heights are highest in this season. Additionally, deciduous trees have not leafed-out, allowing surface conditions to be viewed.

During the summer, canopy closure is more complete and the soil is mostly dry.

2) The class of forest/shrub-scrub wetlands in the classification includes deciduous species. Wet evergreen woodlands cannot be separated from dry evergreen woodlands in either season.

3) The category of intermittent exposed streams as included in the ground truth map of wetlands cannot be identified with Landsat because of the features' small size.

The Tape

The tape is 9-track, 800 B.P.I., and contains 5 files separated by End-of-File marks. All records are 240 bytes in length. The first file contains a single "header" record in EBCDIC format which describes the subsequent files' characteristics. Files 2, 3, 4, and 5 contain the classification results stored as EBCDIC symbols. Each file contains 224 records. File 2 contains potential wetlands classification for April 13, 1977. File 3 contains definite wetlands classification for April 13, 1977. File 4 contains potential wetlands classification for June 26, 1975. File 5 contains definite wetlands classification on June 26, 1975.

For the potential wetlands classifications (files 2 and 4) the symbol '1' represents potential wetlands; '-' represents non-potential wetlands.

For the classification of definite wetlands on April 13 (file 3), '-' represents non-wetland, '1' represents open water, '2' represents emergents, and '3' represents forest/shrub-scrub wetlands.

For definite wetlands on June 26 (file 5), only open water is identified as '1'. Non-wetlands are represented by '-'.

Conclusions

These investigations have contributed to the development of U.S. Army Corps of Engineers applications of current Landsat data. Highlights of the studies include the GISS algorithm performing the best is a comparative study of classification algorithms on the Nebraska Wetlands study and the innovation of a new analysis concept for snow cover applications. This cooperative effort has proven highly productive and will continue during 1982 with emphasis being placed on refinement of the snow cover analysis technqiues.

D. Agro-Environmental Application of Satellite Remote Sensor Data

During 1981 GISS/Columbia staff members continued pursuit of additional applications of satellite remote sensor data to selected projects of personal interest and that support their educational and professional objectives. In general, these studies address specific questions of interest to geographers which will also contribute to increased knowledge of numerical remote sensor data. Presentation of this research has occurred at regional and national meetings of the Association of American Geographers as well as at the NASA/NOAA cosponsered Remote Sensing Educator's Conference (CORSE-81) held at Purdue University (Appendix A).

Landscape "Greenness"

Helene Wilson has proposed that Landsat observations provide a unique and universal measure of landscape vegetated condition, called landscape "greenness". Considerable research has been conducted in agricultural applications of Landsat data that shows a strong relation between various attributes of crop canopies (e.g., percent ground cover, leaf area index, biomass) and various transforms of the Landsat visible and near-infrared observations. Although it has not been proven, this approach to Landsat data would appear to be generally applicable to all landscapes. That is, the degree to which a landscape is vegetated should be related to its "greenness"

as observed by one or more vegetation indices derived from Landsat observations.

Helene has selected a study site in the Hartford, Conn. region, where a complex variety of land cover conditions including forest, agriculture, and urban are present. Her hypothesis is that regardless of the cover type, one or more of the Landsat-derived vegetation indices will indicate the degree to which the landscape is occupied by photosynthesizing vegetation. If this is true then Landsat data can be used as a universal measure of landscape conditions where the vegetation "greenness" may serve as an indicator of current environmental conditions.

During 1981 Helene acquired low altitude color infrared stereo photography and conducted a field measurements program to evaluate the relation between ground conditions and the air photo observations. The aerial photography will provide Landsat subpixel measures of percent area covered with living vegetation and vegetation height. Through intensive analysis of the photography she will establish the vegetated conditions within Landsat observations of various land cover conditions. Through comparison of the photo-derived observations and the Landsat Data, she will test the research hypothesis.

Albedo Studies

Chris Brest, during 1979 and 1980, collected field measurements of the reflectance of building roof tops and parking lots in the Hartford, Conn. region. These observations are being used to calibrate a set of 28 Landsat observations of the Hartford region acquired between 1972 and 1978 and covering eleven months of the year. Calibration of these data to percent reflectance and the combination of Landsat visible and near-infrared measurements provides a good estimate of surface albedo. This further permits

analysis of urban-rural albedo differences as a function of season and cover type. Albedo has been suggested as a significant factor in causing urban/rural climate differences. Chris's analysis will evaluate this hypothesis.

A preliminary analysis of the data (Appendix A) has confirmed that the calibration procedure is effective (error rate of 2-3%) and that urban-rural albedo differences may be smaller (approximately 5%) than is frequently reported. This appears to be related to the inverse variation of visible/near-infrared reflectance through the season; a phenomenon generally not investigated in albedo studies. During 1981 Chris completed analysis of the entire 28 Landsat observations and is currently drafting his research results for submission to the Department of Geography faculty as his doctoral dissertation.

Michael Miller has approached derivation of surface albedos from Landsat data through numerical modelling of atmospheric radiative transfer. By calculating the effects of scattering, as described in the U.S. Air Force Cambridge Laboratories research, and absorption, as described in the Smithsonian Tables, he evaluates the relation between ground reflectance and observed Landsat radiance. Seasonal variations in atmospheric conditions are considered but not short term meteorological conditions.

Michael has applied the model to Landsat observations of eastern Long Island, N.Y. where diverse land cover conditions present a variety of surface albedos. The results, although promising, suggested that his method for handling atmospheric absorption of radiation is less realistic than desirable. The albedos calculated are the right order of magnitude but appear to be overestimated. Using only the scattering model he derives more reasonable

figures. He is currently drafting his research results for submission, as his master's thesis, to the Department of Geography.

Kenyan Agricultural Systems

Tina Cary is conducting a study of agricultural systems in western Kenya (east Africa). Her hypothesis is the Landsat observations record regional variations in the agricultural systems present. In particular, she proposes that, because of striking regional variations in the intensity of agricultural development and regional variations in and interaction between cultural and physical factors that effect local agricultural practices, Landsat observations may be used as an indicator of the agricultural system present in a location.

To identify the relation between regional variations of agricultural systems and Landsat observations she will examine the numerical properties of spatially aggregated Landsat data. Through analysis of the data at various levels of aggregation she will seek to isolate those scales (or resolutions) at which various cultural and/or physical factors are most highly related to landscape appearance. Tina will use this information to develop a systematic approach to landscape regionalization which will permit analysis of the regional patterns of agricultural systems.

During 1982 Tina will travel to Kenya, under a Fullbright scholarship, to conduct field observations to support her analysis. She will be in the field for one year traversing the 10,000 square mile area that represents her study site. The study site consists of the nominal ground coverage of one Landsat scene and thus represents an ambitious field project. Because of her previous field experience in Kenya with Dr. Frank Conant of Hunter College, Tina should be highly successful in accomplishing her objectives.

Conclusions

The diverse research projects undertaken by Columbia students in agro-environmental research provide major contributions to the GISS/Columbia research program with a minimum cost to NASA. The activities in general, do not draw heavily of the group resources and often, as in Tina's case, are significantly supported by other funding sources. However, the outcome of the research significantly contributes to advancing understanding of satellite earth observations. The success of these projects are dependent on the working relation between GISS and Columbia scientists and demonstrate the productive nature of the cooperative agreement.

References Cited

AgRISTARS, 1981. AgRISTARS Annual Report - Fiscal Year 1980, NASA, Johnson Space Center, Houston, Texas.

Baker, J.R. and E.M. Mikhail, 1971. Geometric Analysis and Restitution of Digital Multispectral Scanner Data Arrays. LARS Information Note 052875, LARS-Purdue University, West Lafayette, Indiana.

Barrnett, T.L., 1980. "Recalibration of FSS Data", NASA-JSC Memorandum to D. Pitts. Johnson Space Center, Houston, Texas.

Bauer, M.E., M.C. McEwen, W.A. Malila, and J.C. Harlan, 1978. "Design, Implementation, and Results of LACIE Field Research", Proceedings of the LACIE Symposium, Vol. II. Johnson Space Center, Houston, Texas, Oct. 23-26, 1978, pp. 1037-1066.

Biehl, L.L., 1979. "Algorithm for Detecting Scans for Field Average Version of NASA/JSC Field Spectrometer System (FSS) Data, Memorandum dated 8/22/79 from LARS-Purdue University, West Lafayette, Indiana.

Engel, J.L., 1980. "Thematic Mapper = An Interim Report of Anticipated Performance" Enclosure 5 in NASA Applications Notice "Landsat-D Image Data Quality Analysis Program 10/23/81, Goddard Space Flight Center, Greenbelt, Maryland.

Hyde, R.F., S.N. Goward and P.W. Mausel, 1977. "ISURSL Levels Classification: A Low Cost Approach to Multispectral Data Analysis", Proceedings of the 1977 Machine Processing of Remotely Sensed Data Symposium, Purdue University, West Lafayette, Indiana, pp. 322-331.

LARS (Laboratory for Agricultural Remote Sensing), 1968. "Remote Multispectral Sensing in Agriculture," Vol. 3, Research Bulletin No. 844, Agricultural Experiment Station, Purdue University, West Lafayette, Indiana, Cited in P.W. Swain and S.M. Davis, editors, 1978, Remote Sensing the Quantitative Approach, McGraw-Hill, New York, NY, p. 14.

NASA, Johnson Space Center, 1978, Data Format Control Book, Airborne Instrumentation Research Program, Experiments Systems Division, Oct. 1978. NASA/JSC, Houston, Texas.

NASA/JSC, USDA/ESS, 1979. Enumerator's Manual, 1979 AgRISTARS Ground Data Survey, Johnson Space Center, Houston, Texas.

ORI, 1981. Renewable Resources Thematic Mapper Simulator Workshop, 2/23/81, prepared for NASA/GSFC, ORI, Silver Spring, Maryland.

Richard, R.R., R.F. Merkel, and G.R. Meeks, 1978. "NS001MS - Landsat D - Thematic Mapper Band Aircraft Scanner", Proceedings of the 12th International Symposium on Remote Sensing of Environment, Manila, Philippines, April 1978, pp. 719-728.

Spencer, M.M., J.M. Wolf, and M.A. Scholl, 1974. "A System to Geometrically Rectify and Map Airborne Scanner Imagery and to Estimate Ground Area". NASA Contractor Report, prepared by Environmental Research Institute of Michigan, Ann Arbor, Michigan.

ABSTRACTS OF PAPERS PRESENTED BY COLUMBIA/GISS STAFF

at the

ASSOCIATION OF AMERICAN GEOGRAPHERS ANNUAL MEETING

April 19-22, 1981

Los Angeles, California

DYNAMICS OF SURFACE ALBEDO by Christopher L. Brest

This study assesses the role of albedo as a contributing factor to the formation of urban heat islands. Field spectroradiometric measurements are used to calibrate twenty-seven Landsat observations of the Hartford, Connecticut region. Calibration of these remotely sensed data permits analysis of the spatial and temporal variations of surface albedo for the entire region. The study investigates albedo differences between man-made urban surfaces and natural vegetative surfaces. Additionally, spectral reflectance in the visible and near-infrared are being studied to determine their contribution to net shortwave albedo.

SEASONAL TRENDS IN LAND COVER ALBEDO ON EASTERN LONG ISLAND by Michael S. Miller

Land cover albedo is evaluated using multitemporal Landsat MSS data. This is accomplished by applying the Elterman atmospheric attenuation model. Temporal variations in incoming radiation at the surface are first determined with the model and compared with ground pyranometric measurements. Assuming 100 percent reflection, the model is used to estimate radiation reaching the satellite sensor. The ratios of Landsat energy measurements to these estimates are used to derive albedo values. The Riverhead, Long Island study site includes agriculture, oak forest, pine barrens, water, and urbanized lands. These land cover types are examined for spatial and seasonal variations in surface albedo.

PATTERNS OF AGRICULTURE: A FUNCTION OF SCALE by Tina K. Cary

Studies in agricultural geography have generally occupied two extremes on a scale continuum: detailed field mapping, and large-area regionalization. The opportunity now exists to investigate spatial patterns of agriculture at meso-scales as well, using the Landsat data base. In this study, patterns of agriculture in the tropical highlands of western Kenya are being investigated for a range of scales. Landsat digital data are spatially aggregated to generate the range of scales. Using this approach, the gap in the scale continuum can be bridged, permitting explicit consideration of how patterns of agricultural land use appear to vary with scale.

LANDSAT MEASUREMENT OF LANDSCAPE GREENNESS by Helene Wilson and Samuel N. Goward

The principal information contained in Landsat multispectral data is the degree to which any landscape is occupied by photosynthesizing surfaces and is expressed in the relative differential between visible and near-infrared radiances. Numerous studies have demonstrated the utility of vegetation indices based on this differential for assessing a variety of land cover conditions. This investigation extends previous work by explicitly relating the amount of actively producing vegetation cover within a pixel to recorded radiances for a heterogeneous landscape. The "greenness" approach offers potential as a nomothetic solution to the problem of exploiting the uniquely global features of Landsat observations.

Paper presented at 1980 Annual Meeting,
Association of American Geographers Middle States Division,
University of Delaware, Newark, Delaware, October, 1980

OBSERVATION OF URBAN/RURAL ALBEDO CONTRASTS

Christopher L. Brest and Samuel N. Goward*

Columbia University

*Columbia University and NASA Goddard Institute for Space Studies

INTRODUCTION

Since albedo is a significant determinant of net radiation it has been suggested that the modified urban climate may be due to the differences in albedo of urban and rural surfaces. This research is an investigation of variations in surface albedo in the Hartford, Connecticut region. The intent of the study is to assess urban/rural surface albedo differences and to ascertain the seasonal variability of these differences.

It is hypothesized that the albedo of a mid-latitude city in a humid climate is significantly lower than that of its surrounding rural environs. The higher albedo of the rural area is attributed to vegetation in the summer and snow cover in the winter. It is further hypothesized that the urban/rural differences vary seasonally due to changes in rural albedo.

The methodology employed in this study allows measurement of the albedo of the entire study site, not just 'representative' samples. Urban areas are mosaics of various man-made and natural surfaces and only by a study of the entire region can an understanding of the spatial and temporal characteristics of albedo be acquired. Until recently equipment and techniques have not been available to undertake the type of study proposed here. Use of remote sensing techniques avoids the problem of spot measurements or representative samples. The utility of remotely sensed, image formatted data to measure solar and terrestrial radiation values has been demonstrated [1,2,3,4].

AVAILABLE DATA

The primary data for this study consists of 25 observations of the Hartford, Conn. area acquired between 1972 and 1978 by the Landsat multispectral scanner. The data are available in digital form and are being analyzed at NASA's Goddard Institute for Space Studies. The 25 observations give excellent seasonal coverage. The number of observations per month are shown below:

JAN.	FEB.	MAR.	APR.	MAY	JUN.	JUL.	AUG.	SEP.	OCT.	NOV.	DEC.
2	3	2	1	1	3	2	4	2	4	1	-

Additional data includes the radiometric measurements of selected urban targets collected by the authors which are to be used in the calibration procedure.

RESEARCH DESIGN

To successfully determine surface albedo from spectrally selective, remotely sensed satellite observations three questions must be addressed:

1) How do you derive albedo from spectral measurements?

2) How do you convert radiance to percent reflectance?

3) How do you account for atmospheric effects?

Albedo is defined as the ratio of reflected to total radiation in the short wave portion of the spectrum ($<4.0\ \mu m$)[5]. It is therefore necessary to consider the reflectance of the surface in this entire range. Spectral intervals must be chosen which are representative of reflectance in this range. This necessitates a knowledge of the reflectance characteristics of the surfaces involved. Man-made surfaces such as concrete and asphalt display a fairly constant reflectance with changing wavelength. Vegetation has a very distinct reflectance curve, with a significant rise centered

at about 0.725 μm separating the response of vegetation into two distinct segments: low reflectance in the visible and high reflectance in the near-infrared. This variation in reflectance of a vegetative surface is accounted for in this study by constructing a weighted average of the reflectance in the visible and near-infrared. The weighting factors, 60% for the visible and 40% for the near-infrared, are derived from the proportion of incident solar radiation which lies below and above the vegetation rise at 0.725 μm[6].

The Landsat multispectal scanner operates in four spectral intervals: 0.5-0.6, 0.6-0.7, 0.7-0.8, 0.8-1.1 μm. The use of two Landsat bands which straddle the rise in vegetation reflectance can be employed to construct an accurate albedo measurement from Landsat spectral observations.

The issues raised by the last two questions stated above are accounted for by the calibration procedure used in this study. The methodology employed utilizes a radiometer which provides multispectral reflectance readings of selected sites in the form of percent reflectance. The radiometer was designed specifically to provide these readings in support of remote sensing missions and is described elsewhere[7]. Once computed the percent reflectance of the targets is independent of atmospheric conditions. This is an important feature because once a target has been measured, it can be utilized in the calibration of satellite observations from different passes. It eliminates the need to have ground based measurements taken coincidently with each satellite pass. A necessary condition for the success of this procedure is that the targets selected must be temporally stable. The targets chosen are large man-made surfaces: building roofs and parking lots. This will test a new type of target not previously used in calibrating satellite data.

For this preliminary paper 14 targets whose reflectances were measured in the summer and fall of 1979 are being used. Field work is continuing in the summer of 1980 to increase the number of calibration targets. The 14 targets range from dark to bright: percent reflectances from approximately 4 to 50%.

The radiometrically observed spectral reflectance measurements are used to calibrate the satellite data. Regression analysis is used to determine the relationship between ground and satellite observations of the targets sites (Fig. 1). Each band is calibrated separately to transform the satellite observed radiances to reflectance and to remove atmospheric effects. The two bands are combined according to the weighted average previously discussed. Calibrated albedo maps can now be produced either in the form of computer printouts or video display.

PRELIMINARY RESULTS

Using the data from the 14 targets we began to evaluate our research design using 4 of the 25 satellite passes as representative of the seasons. The statistical relationships are shown below:

TARGET LANDSAT STATISTICAL RELATIONSHIPS
(Measured percent reflectance vs. Landsat radiance)

		MAY	AUG	NOV	FEB (No snow cover)
EXPLAINED VARIANCE (R^2)	BAND 4 (Visible)	0.90	0.89	0.90	0.90
	BAND 6 (Near IR)	0.83	0.86	0.88	0.86
STANDARD ERROR OF ESTIMATE (% REFLECTANCE)	BAND 4	2.6	2.8	2.6	2.6
	BAND 6	3.9	3.3	3.2	3.5

The R^2 values (0.83-0.9) are highly encouraging and indicate the potential of our procedure for calibrating satellite data. The standard error of estimate is higher than we had hoped but we are confident that this can be lowered to approximately 1% through the addition of more calibration targets.

Determination of the albedo of natural versus man-made surfaces was conducted using the USGS landuse-landcover classification 1:250,000 scale map of Hartford. For purposes of this paper we have selected six land-cover types to demonstrate our preliminary conclusions. They are:

DR = Dense Residential

LR = Low Density Residential

CD = Commercial,Industrial,Transportation (Downtown)

A = Agriculture

F = Forest

WN = Wetland,Nonforest

In general, albedos of man-made surfaces are lower than those of vegetative surfaces. The seasonal variation of albedo for the six land-cover types is shown in Fig. 2. The variation is the greatest for the landcover types which have a high proportion of vegetation, i.e., A,F,WN, LR. The landcover types which are comprised mainly of man-made surfaces are lower and have much less seasonal variation. The driving force behind these albedo differences is the high infrared reflectance from vegetation foliage. Reflectance in the near-infrared also shows seasonal variation. It is this high reflectance in the infrared which produces the summertime peak in the seasonal albedo shown in Fig. 2. This point is further reinforced by looking at Fig. 3 which shows the ratio of BAND 6/BAND 4. There exists a high ratio in the spring and summer. The LR landcover type falls into this grouping because of the large proportion of vegetation present

between the man-made structures.

The three landcover types which might be considered 'urban' are shown in Fig. 4. This figure shows the individual band reflectances for the three types. Again the type with the highest proportion of vegetation, LR, has a much higher reflectance in the infrared during spring and summer and is more variable. Notice the relative uniformity of the two landcover types comprised mainly of man-made surfaces, CD and DR, during the course of the year.

Color video displays of the computer generated albedo maps clearly demonstrate the considerable seasonal dynamics of landcover albedos. Rural, vegetative, surfaces have a high albedo in spring and summer. Urban areas, or those comprised mainly of man-made surfaces, have a lower albedo and remain more consistent throughout the four passes. In the fall and winter rural surfaces return to a lower albedo, similar in magnitude to that of urban areas.

At the present time the albedo values derived are low in comparison with those stated in the literature. The reason for this may be the calibration panel which is used to derive the percent reflectance values for the targets. We believe the furnished percent reflectance value for the panel is too low. At the conclusion of the summer 1980 field measurements program the panel will be sent out for laboratory testing to confirm this suspicion.

CONCLUSIONS

Results generated demonstrate that seasonal variation in rural albedo is significant. To understand urban/rural albedo contrasts seasonal

variations must be studied. Certain technical limitations in the calibration procedure need to be resolved before the absolute magnitude of urban/rural albedo contrasts can be assessed. The methods applied in this research show great promise in providing appropriate data for analysis of both temporal and spatial variation of surface albedo. Final results of this research should provide a valuable contribution to studies of variations in interface energy budgets that result from variable land-cover conditions.

ACKNOWLEDGMENTS

The authors are grateful to Prof. Francis Conant of Hunter College, C.U.N.Y., for the generous loan of the field radiometer. This research was supported in part by NASA grant NSG-5080.

REFERENCES CITED

[1] Robert W. Pease and David A. Nichols, "Energy Balance Maps from Remotely Sensed Imagery," Photogrammetric Engineering and Remote Sensing 42 (November 1976): 1367-73.

[2] Robert W. Pease et al.,"Urban Terrain Climatology and Remote Sensing," Annals AAG 66 (December 1976): 557-69.

[3] William A. Malila, "Radiation Balance Mapping With Multispectral Scanner Data," Remote Sensing of Earth's Resources Vol. 1 (1972): 769-83.

[4] Robert H. Alexander et al., Applications of Skylab Data to Land Use and Climatological Analysis, Final Report Skylab/EREP Investigation no. 469 Reston, Virginia: U.S. Geological Survey, 1976.

[5] William D. Sellers, Physical Climatology (Chicago: University of Chicago Press, 1965), pp. 19-20.

[6] Robert W. Pease and Stephen R. Pease, Photographic Films as Remote Sensors for Measuring Albedos of Terrestrial Surfaces, Technical Report V, U.S.G.S. Contract 14-08-0001-11914, University of California, Riverside, 1972.

[7] Dwight D. Egbert, Spectral Reflectivity Data: A Practical Acquisition Procedure, University of Kansas, Center for Research, Inc. 1970.

ABSTRACT

In this study an examination is made of spatial and temporal variations of urban/rural albedo in the Hartford, Conn. region. Such contrasts have been proposed as one cause of observed differences in climatic phenomena. Due to the complexity of ground cover, the determination of spatial variability of surface albedo is difficult with with traditional ground based observations. In this study calibrated Landsat acquired remote sensor measurements are used for albedo assessment. Results indicate that urban/rural albedo differences vary temporally. This results primarily from seasonal changes in the reflectance properties of vegetation canopies. Greatest albedo differences between urban and rural areas occur during the summer due to the high near-infrared reflectance by vegetation. The smallest differences occur during the winter, with the absence of snow.

FIG. 1 SCATTER PLOT OF LANDSAT BAND COMPARED TO TARGET REFLECTANCE VALUES (BAND 4, MAY)

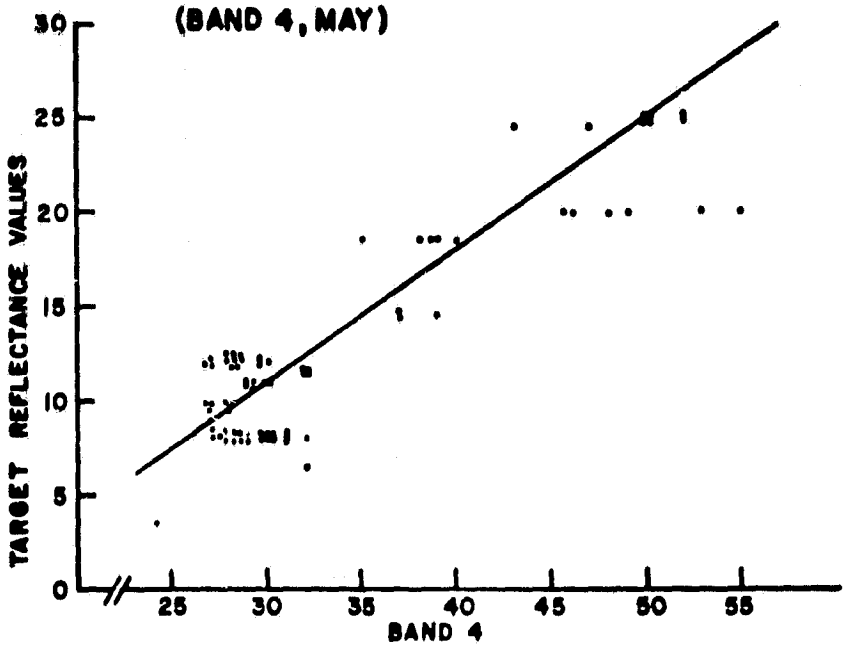

FIG. 2 SEASONAL VARIATION OF ALBEDO

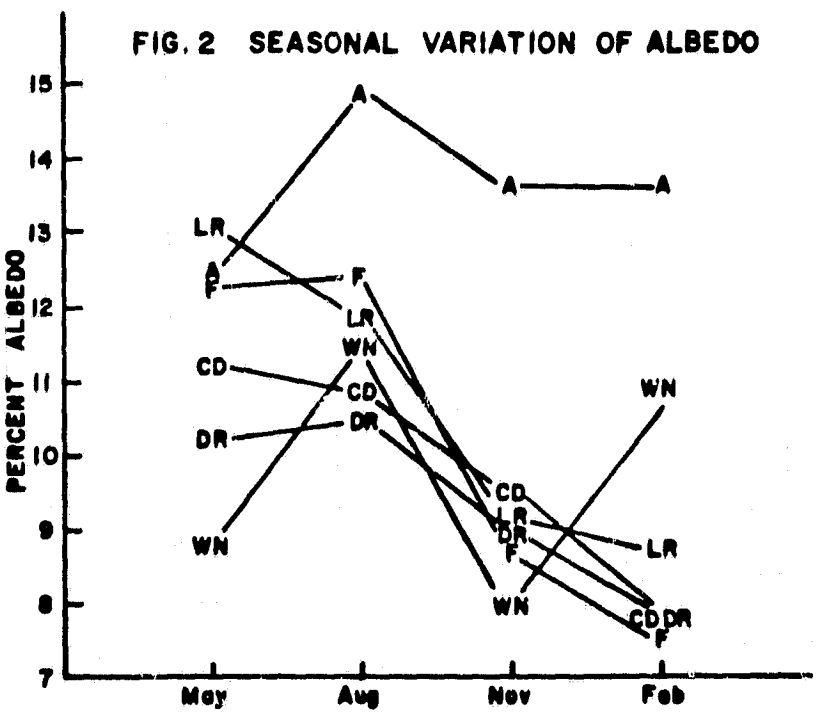

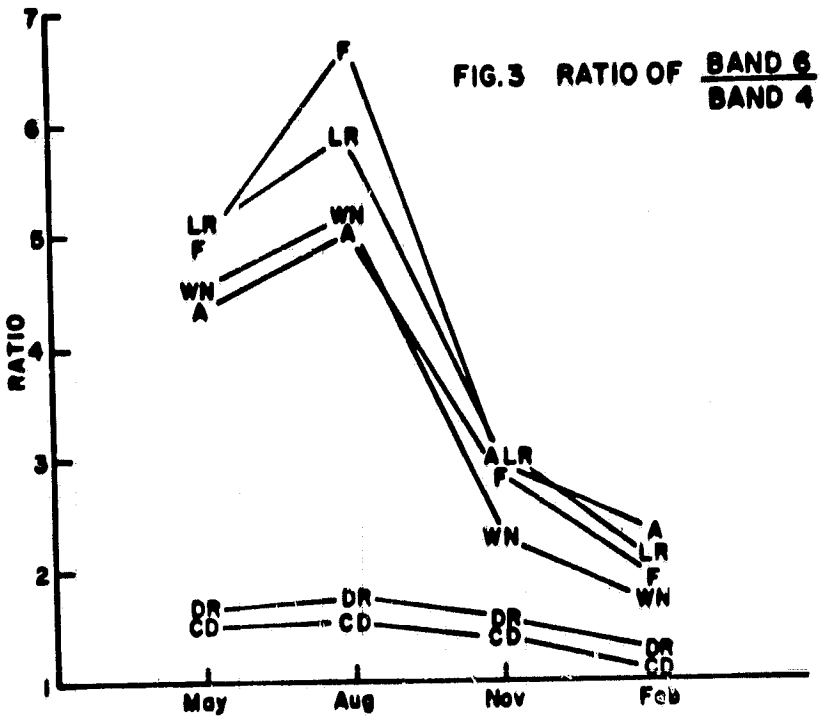

FIG. 3 RATIO OF $\frac{\text{BAND 6}}{\text{BAND 4}}$

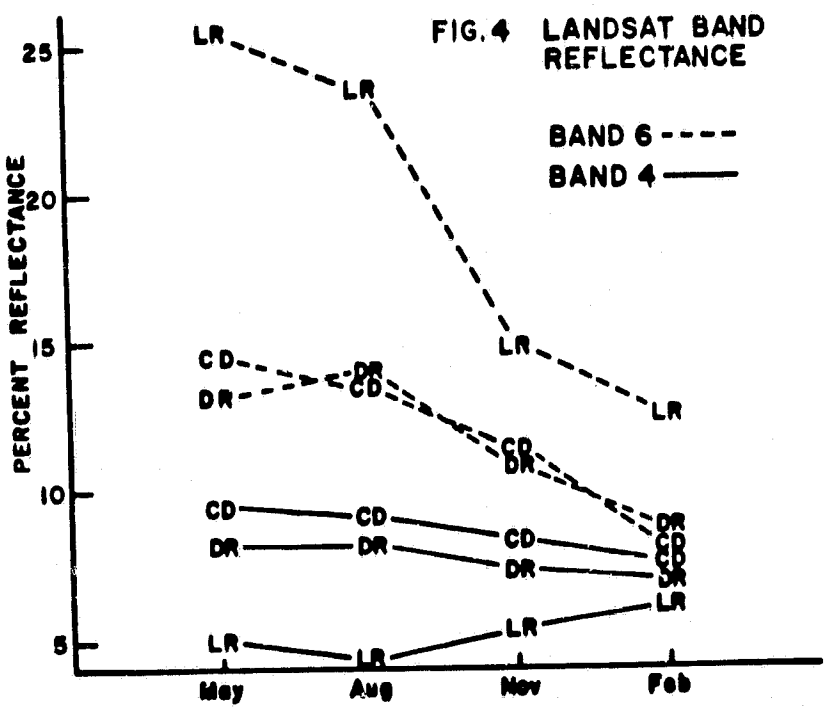

FIG. 4 LANDSAT BAND REFLECTANCE

BAND 6 - - - -
BAND 4 ——

CORSE-81

The 1981 Conference On Remote Sensing Education
May 18-22, 1981 Session No. 4C

REMOTE SENSING RESEARCH IN GEOGRAPHIC EDUCATION: AN ALTERNATIVE VIEW

Helene Wilson, Tina K. Cory, and Samuel N. Goward
Department of Geography, Columbia University
and
NASA/Goddard Institute for Space Studies

THE PROBLEM

Geography currently plays a major role in remote sensing education in this country (Estes, et al., 1977), with the emphasis today on training students in the application of remotely sensed observations to geographic problems. This emphasis reflects a prevailing view of remotely sensed data interpretation as a well-established body of techniques to be applied in solving a broad spectrum of geographic problems. This view is also apparent in what we see as the current emphasis in geographic remote sensing research on applications studies. The underlying assumption of this applications orientation is that the information content of remotely sensed data is known and coincides with the types of information required for particular purposes.

There is some question as to the degree to which analysis of contemporary remotely sensed data for applications purposes is satisfactory. The categories of information typically of interest in applications work (e.g., Anderson, et al., 1976) have not proved to be interpretable from current remotely sensed data with consistency and confidence. This situation raises doubts as to the degree to which the information contained in the current generation of sensor observations of the earth's surface is understood.

SOURCE OF THE PROBLEM

Modern remote sensing systems have been criticized by some investigators as not being effective in providing the types of information for which the use of traditional observation systems (e.g., aerial photography) has been proven successful. While this criticism may be viewed as merely a conservative reaction to the appearance of new technology, it is a valid criticism. The advent of remote sensing from space occurred during a period in which American geographical photointerpretation work emphasized applications (Stone, 1974). Investigators appear to have turned to the new data as another means of solving the same types of geographical problems to which they had been

applying aerial photography. There was no phase of theoretical investigation of these new data comparable to that which had preceded the applications phase in aerial photographic interpretation.

Not surprisingly, investigators have encountered difficulties in addressing a set of problems that have remained the same with data that have changed markedly. The spatial, temporal, and spectral/radiometric parameters of new observation systems are significantly different from those of what may now be regarded as "traditional" systems. The major innovations associated with remote sensing from space are as follows:

1) spatial: uniform observations are acquired on a global scale, and are more generalized;
2) temporal: coverage is of significantly higher frequency;
3) spectral/radiometric: observations are numerical measurements, in many wavelength bands.

These features have a number of implications for the extraction of geographic information from these new data. For example, the spatial resolutions typically encountered in these new data are coarser than those characteristic of most aerial photography. The relationship between images in photography and features on the ground is fairly well understood as a result of accumulated experience in extending visual perception of the surface to aerial perspectives. However, there is no reason to assume that the associations which can be made at one scale are valid at another. Furthermore, sensor systems do not necessarily generalize landscapes in ways consistent with our conceptual or cartographic generalizations. Similarly, the increased temporal resolution possible with satellite observing systems is quite different from that of "traditional" systems. Aerial photographic missions are usually planned for a time of year considered to be optimal for a particular application (e.g., tree identification), and repeat coverage is rarely obtained more than once every five years. As a result, the selection of an appropriate observation date from among the many available for a given geographic location becomes problematical with these new data.

Analysis of remotely sensed data in numerical format has been put forward as a possible solution to some of the difficulties presented by the characteristics of these new observations. In particular, analysis of the numerical data at the resolution limit of the sensor and utilization of all wavelength bands simultaneously has been expected to provide information about the surface in greater detail than that which human beings are able to extract from visual assessment of imagery. Automated interpretation has also been seen as a means of efficiently utilizing a data base that has been accumulating with unprecedented rapidity.

The spectral signature paradigm, widely employed in computer-based interpretation of the multivariate, numerical data, has not met with resounding success. For example, a survey (Joyroe, 1978) of investigations using digital Landsat data to classify land cover indicates that classification accuracy figures are on the average significantly lower than the minimum criterion of 85 percent often used for visual image interpretation (Anderson, et al., 1976). Furthermore, spectral signature methods give acceptable results only over very limited areas and only at certain times. In addition, these methods nearly always require significant amounts of ancillary ground information. As a result, automated interpretation has yet to be proven as a means of exploiting the global and temporal coverage afforded by satellite data. Apparently, the numerical analysis techniques in wide use are unable to address effectively the problems raised by the features of contemporary remotely sensed earth observations.

We believe that others, like ourselves, have found that the results of analysis of these new data have not conformed to initial

expectations. However, we do not believe that these new observation systems should be rejected. We suggest that the problem lies in our limited understanding of the nature of the data now being acquired. A comprehensive understanding of the spectral, spatial, or temporal properties of landscapes, as observed with contemporary earth observation systems, has not yet been developed.

WHAT NEEDS TO BE DONE?

We see a need for basic research to determine the inherent information content of the data. An approach that we propose is to consider remotely sensed data as a measure of one or more unknown or poorly-understood landscape attributes. The hypotheses for this research should originate in examination of the remotely sensed data rather than from external objectives. The goal of this research is to establish models of landscapes that may be used to explain the information content of remotely sensed data.

One hypothesis that should be investigated is whether remotely sensed observations provide measures of continuously distributed landscape physical attributes -- for example, moisture content, thermal inertia, and chlorophyll content -- rather than simply indicating the presence and extent of discrete categories or objects. To test this hypothesis requires a thorough knowledge of the interactions between electromagnetic energy and landscapes, as expressed in the spectral/radiometric component of remotely sensed data. Study of these interactions is prevalent in remote sensing research conducted in the non-photographic regions of the electromagnetic spectrum. For example, microwave remote sensing research is concerned with the influence of moisture on observations; thermal properties are considered to be key landscape attributes in explaining thermal infrared observations. This approach is not often taken in the peak energy range of the solar spectrum (visible and near-infrared), because data such as those acquired by the Landsat system tend to be viewed as merely an extension of what is already known from experience with photographic observations. However, we believe that this presumption is not correct. New remotely sensed data cannot be viewed simply as a direct extension of our visual capabilities.

Additional study is needed to investigate the relationships between radiometric measurement of landscape attributes and spatial and temporal factors. For example, one hypothesis might be that the ability to measure a particular landscape attribute is invariant as a function of the spatial resolution of the observing system. Although one might expect different attributes to be measurable at different scales of observation, relatively little is known about the ways in which sensors generalize the surface as a function of observation cell size. If the ability to measure a particular attribute is found to vary with scale, then a new focus for investigation becomes the determination of the scale range over which the attribute is measurable.

With respect to temporal factors, an initial hypothesis that should be examined is that a given landscape attribute is measurable at all times. The consistency and precision of that measure may in fact vary with time -- for example, because of variations in factors external to the landscape, such as seasonal differences in intensity of solar radiation.

WHO SHOULD DO THIS RESEARCH?

Specialists in many disciplines have contributed to advances in remote sensing of the earth's surface, including engineers, mathematicians, physicists, agronomists, geologists, and others. However, investigators in each of these disciplines understand and are concerned with only a part of the observed landscape and/or of the data. The data, in contrast, are holistic, in that they represent integrated observations of landscapes. Geography is the discipline that claims an integrated approach to landscapes (Fenneman, 1919). Therefore,

geographers bear a major responsibility for basic research on the remotely sensed observation of landscapes.

While our contention about the unique approach of geographers would meet with little disagreement, the conclusion we draw with respect to the role geographers should be taking in basic remote sensing research is perhaps less widely accepted. Geography as a discipline appears to view itself largely as a passive user of remotely sensed data, principally interested in using the data as an adjunct to current research objectives. The development of analysis techniques, theories, and specifications for future system designs is left to other disciplines. Many geographers view basic remote sensing research as "non-geographic," since it is seen as being concerned with "technique" rather than with what is regarded as substantive geographic inquiry.

This attitude has hindered geographers in making remote sensing research contributions commensurate with the breadth of geographers' perspectives on landscapes. We cannot depend on others to develop theories and paradigms for us. The concerns of the systematic disciplines are not necessarily coincident with our own. Geography is the only discipline which takes an integrated approach to the explanation of areal differentiation on the earth's surface. We routinely apply this approach in attempting to explain field observations and ground measurements. Remote sensing systems provide new observations and measurements of areal differentiation. We must assume our responsibility to seek new theories to explain the data and to provide others with the benefits of our insights.

SIGNIFICANCE OF THIS APPROACH

Remotely sensed observations of the earth's surface raise questions that are particularly geographic in their form and scope. Geographers have contributed significantly to development of aerial photointerpretation techniques by detailed examination of the information contained in the photographs. The new generation of remotely sensed observations has yet to be examined with such rigor. This failure to conduct the needed basic research has constrained our ability to extract and apply the geographic information contained in these new data. We contend that the research approach we are proposing will not only improve applications of these new observations to geographic problems of current interest but will also provide new ways of examining landscapes that may directly contribute to advancement of geographic methodology and theory.

The demonstration that remotely sensed observations of the earth's surface consistently measure selected attributes of landscapes should enable the construction of models that describe the relationships between landscape factors (e.g., spatial arrangement, vertical extent of landscape elements within the observation cell) and the attributes as measured in the data. These models should then serve to enhance the utility of remotely sensed observations for collecting information about the surface. For example, this approach should lead to an improvement in our ability to use the data to identify and map nominal classes by providing a physical basis for explaining and predicting the degree to which any ground category is distinguishable from others present in the landscape. This knowledge should also serve as a guide in the selection of remotely sensed data appropriate to a particular problem. In addition, if the data provide consistent measurements of landscape attributes, nomothetic solutions to the interpretation of the data should be possible which will allow analysis of the data from any geographic location, with a minimum of ancillary information.

The potential of remote sensing as a new source of geographic knowledge about the environment has not been fully exploited (Bowden, 1977). We expect that the attributes measurable with remotely sensed data will serve as new indicators of landscape conditions. For example, if these observations provide a measure of the degree to which a

landscape is photosynthetically active, we have a new means to study the biophysical functioning of landscapes in relation to natural and cultural factors. This integrated expression of landscape dynamics should be highly amenable to modeling, and model refinement should be facilitated by the availability of a large data base against which to test model predictions. The results of this research could lead to significant new geographic concepts that would assist in environmental analysis and resources assessment as well as contribute to advanced understanding of landscapes on a global basis.

IMPLICATIONS FOR REMOTE SENSING EDUCATION

Within many geography departments remote sensing is viewed as a mere "technique" a student should learn in order to carry out "true" geographic research. This view inhibits both students and faculty from investigation of remotely sensed data as a new source of geographic knowledge that may alter our understanding of the earth. The tendency has been for geographers to accept these new data and analysis techniques from engineers and mathematicians without questioning the accompanying premises. This "black-box" approach has hindered geographic applications of the new remotely sensed data and has limited the geographer's contribution to further development of remote sensing observation systems.

We suggest that geographers accept their inherent responsibility to contribute to the development of remote sensing through pursuit of basic research along the lines we have proposed. This research can be encouraged, particularly among students, by demonstrating the links between geographic theory and remotely sensed observations, encouraging a healthy skepticism concerning our current understanding of these data, and suggesting possible avenues of research which may improve our understanding. The incorporation of the framework of inquiry proposed here into current geographic remote sensing research and education presents a challenge. Rising to this challenge will, by bringing the full weight of the geographic perspective to bear on these new observations, contribute to the realization of the inherent value of contemporary and future remote sensing systems. At the same time, pursuit of answers to questions such as those we have posed should enhance our understanding of landscapes.

REFERENCES

Anderson, J. R., E. E. Hardy, J. T. Roach, and R. E. Witmer. "A Land Use and Land Cover Classification System for Use with Remote Sensor Data." Geological Survey Professional Paper 904. Washington, D. C.: U. S. Government Printing Office, 1976.

Bowden, L. "Remote Sensing and Geography." RSEMS 4(1977):17-21.

Estes, J. E., J. R. Jensen, and D. S. Simonett. "The Impact of Remote Sensing on United States' Geography: The Past in Perspective, Present Realities, Future Potentials." Proceedings of the 11th Int'l. Symp. on R. S. of Env't., 25-29 April 1977. Ann Arbor, Michigan: Environmental Research Institute of Michigan, 1977.

Fenneman, N. "The Circumference of Geography." Annals AAG 9(1919):3-11.

Joyroe, R. R., Jr. Some observations about Landsat digital analysis. NASA Technical Memorandum TM 78184. MSFC, Alabama: George C. Marshall Space Flight Center, August 1978.

Stone, K. "Developing Geographical Remote Sensing." In Remote Sensing: Techniques for Environmental Analysis, pp. 1-13. Edited by J. E. Estes and L. W. Senger. Santa Barbara, Cal.: Hamilton, 1974.